Vol. 92 No. 6 pp. 2310–2332 ACTA GEOLOGICA SINICA (English Edition) Dec. 2018

Geological Controls on the CBM Productivity of No.15 Coal Seam of Carboniferous–Permian Taiyuan Formation in Southern Qinshui Basin and Prediction for CBM High-yield Potential Regions

ZHANG Zheng[1, 2, 3, *], QIN Yong[4], ZHUANG Xinguo[1, 2], LI Guoqing[1, 3, 5] and LIU Donghai[4]

1 *Key Laboratory of Tectonics and Petroleum Resources, China University of Geosciences, Ministry of Education, Wuhan 430074, China*
2 *Faculty of Earth Resources, China University of Geosciences, Wuhan 430074, China*
3 *State Key Laboratory of Water Resource Protection and Utilization in Coal Mining*
4 *Key Laboratory of Coalbed Methane Resources and Reservoir Formation Process, Ministry of Education, China University of Mining and Technology, Xuzhou 221116, Jiangsu, China*
5 *State Key Laboratory of Coal and CBM Co-mining, Shanxi Jincheng Anthracite Mining Group Co. Ltd., Jincheng 048000, Shanxi, China*

Abstract: Coalbed methane (CBM) resources in No.15 coal seam of Taiyuan Formation account for 55% of the total CBM resources in southern Qinshui Basin (SQB), and have a great production potential. This study aims at investigating the CBM production in No.15 coal seam and its influence factors. Based on a series of laboratory experiments and latest exploration and development data from local coal mines and CBM companies, the spatial characteristics of gas production of No.15 coal seam were analyzed and then the influences of seven factors on the gas productivity of this coal seam were discussed, including coal thickness, burial depth, gas content, ratio of critical desorption pressure to original coal reservoir pressure (RCPOP), porosity, permeability, and hydrogeological condition. The influences of hydrological condition on CBM production were analyzed based on the discussions of four aspects: hydrogeochemistry, roof lithology and its distribution, hydrodynamic field of groundwater, and recharge rate of groundwater. Finally, a three-level analytic hierarchy process (AHP) evaluation model was proposed for predicting the CBM potentials of the No.15 coal seam in the SQB. The best prospective target area for CBM production of the No.15 coal seam is predicted to be in the districts of Panzhuang, Chengzhuang and south of Hudi.

Key words: coalbed methane, gas productivity, controlling factors, production potential, Taiyuan Formation, southern Qinshui Basin

1 Introduction

With the rapid development of coalbed methane (CBM) in China, the investment in CBM has increased significantly in recent years (Qin et al., 2018). The Qinshui Basin is the largest CBM producing basin in China with approximately 4.0×10^9 m^3 annually derived from the CBM reservoirs of the Carboniferous–Permian Taiyuan Formation and Shanxi Formation. By the end of the year 2015, as many as 10060 CBM wells had been drilled in the Qinshui Basin, and among these wells 7100 are producing wells (Ye Jianping and Lu Xiaoxia, 2016). The most successful CBM commercial development regions in the Qinshui Basin are occurring in the southern portion, where the CBM production accounts for more than 90% of the total production of the entire Basin (Zhang et al., 2018). Due to shallower burial depth, higher gas saturation and permeability, and mature CBM development technology of No.3 coal seam, the CBM exploitation in southern Qinshui Basin (hereafter referred to as SQB) has always been over-dependent on No.3 coal seam in Shanxi Formation these years (Ye jianping et al., 2009; Lv et al., 2012; Zhang Zheng et al., 2015), accordingly, the influencing factors of CBM enrichment and gas production of this seam, such as burial depth, coal

* Corresponding author. E-mail: zhangzheng@cug.edu.cn

thickness, gas content, porosity, permeability, structural setting and hydrologic condition and so on, have been extensively studied by numerous scholars (Cai et al., 2011; Lv et al., 2012; Liu et al., 2012; Tao et al., 2014; Wang et al., 2015). Compared with No.3 coal seam, the No.15 coal seam in the Taiyuan Formation in SQB has lower gas saturation and permeability, higher water production, and looser coal structure (Ye jianping et al., 2009), which are unfavorable for CBM development. Thus, the investment on the CBM exploration and development of No.15 coal seam were relatively lower over the years, and there are very few targeted researches on the gas production and its corresponding controlling factors for the No.15 coal seam, and only some studies on the geology related to CBM of No.15 coal seam in SQB have been conducted (Su et al., 2005; Wei et al., 2007). Nevertheless, the CBM resources in No.15 coal seam account for 55% of the total CBM resources in SQB (Liu Huanjie et al., 1998), more abundant than that in No.3 coal seam. With the commercial development expanding in SQB, the No.15 coal seam must be the potential target seam for CBM development in the next few years. Knowledge of the gas production characteristics and controlling factors of No.15 coal seam will benefit the screening of target areas, the selection of development techniques and the improvement of CBM recovery of this seam in SQB, while our understanding of these two aspects about this seam is still poor.

In this paper, based on our laboratory experiments and the latest exploration and exploitation achievements of local coal mines and CBM companies, the gas production characteristics and the controlling factors of CBM productivity of No.15 coal seam in SQB were discussed, finally, the fuzzy analytic hierarchy (AHP) process was established to screen the best prospective targets for CBM production of No.15 coal seam.

2 Geological Setting

The Qinshui Basin is situated in North China with an area of 2.7×10^4 km^2 (Fig. 1a). It is a large-scale Mesozoic synclinorium with an axis striking NNE–SSW. The study area is located in the southeast of Qinshui synclinorium (Fig. 1b), and the overall structural setting is a monoclinic structure, dipping towards NW (Fig. 1c). The eastern edge of the area is Jinhuo Fault belt striking NNE; Sitou arc-

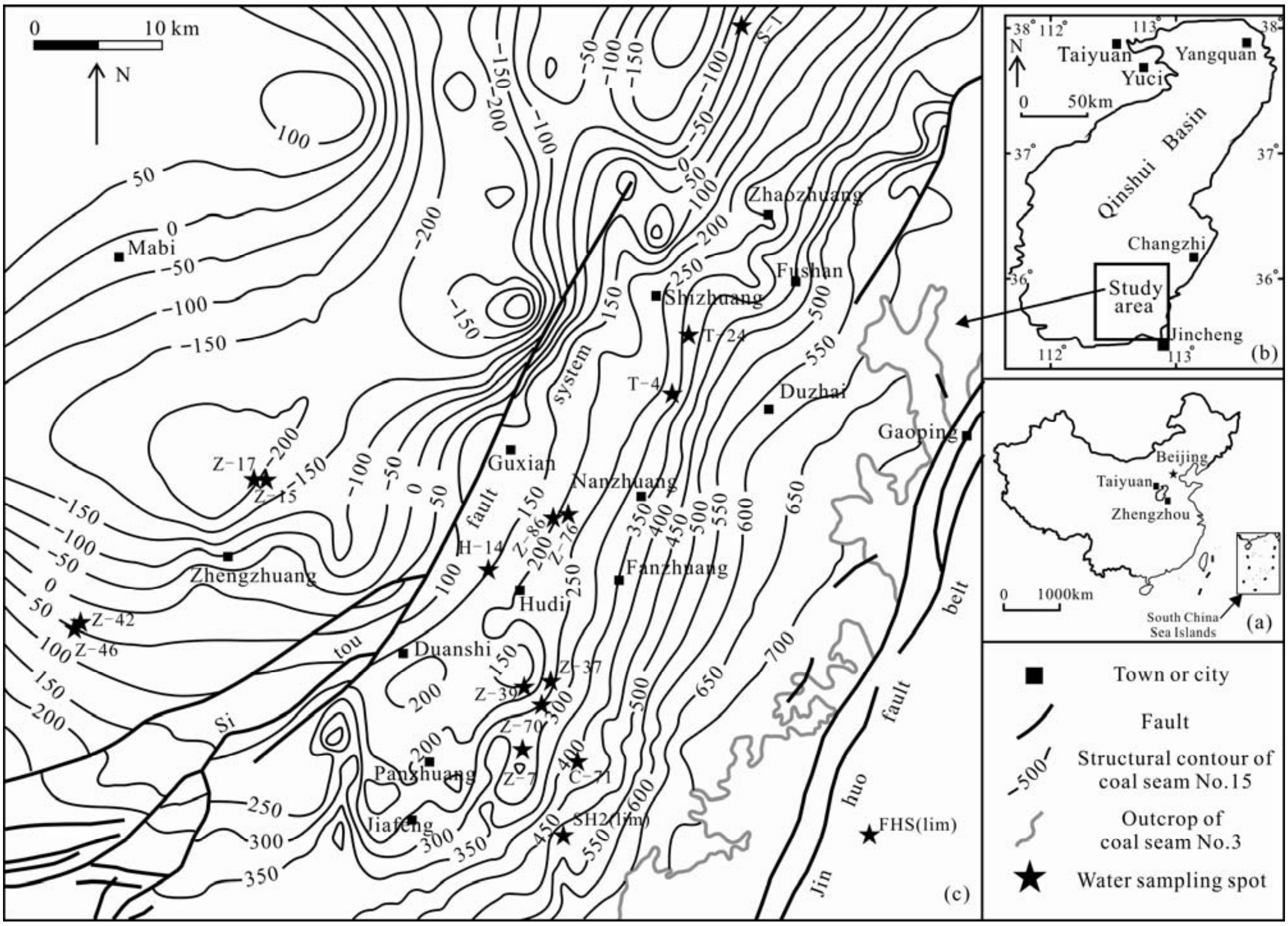

Fig. 1. (a), The location of Qinshui Basin in China; (b), Map of the Qinshui Basin and the location of the study area; (c), Elevation of the bottom of No.15 coal seam with water sampling spot in SQB.

shaped Fault system lying in the center of the area strikes NE. A series of wide and gentle subsidiary folds with an axis striking NNE, NE and SN are widely distributed in the study area. The dip angle of the formation generally varies from 3^{o}–13^{o} (Cai et al., 2011).

The major coal-bearing strata for CBM interest in SQB include Shanxi Formation of the Lower Permian and Taiyuan Formation of the Carboniferous–Permian (Fig. 2). The thickness of the coal-bearing strata varies from 132.44 –166.33 m, with an average of about 150 m; the strata contains more than 10 coal seams, with a total thickness ranging from 3.65–23.8 m. The Shanxi Formation was deposited in a coastal delta environment and principally composed of sandy mudstone, sandstone, mudstone and coal seam; the thickness of Shanxi Formation is between 21 m to 98 m, with an average of about 46.78 m. The Taiyuan Formation was formed in marine-continental transitional facies depositional environments and mainly

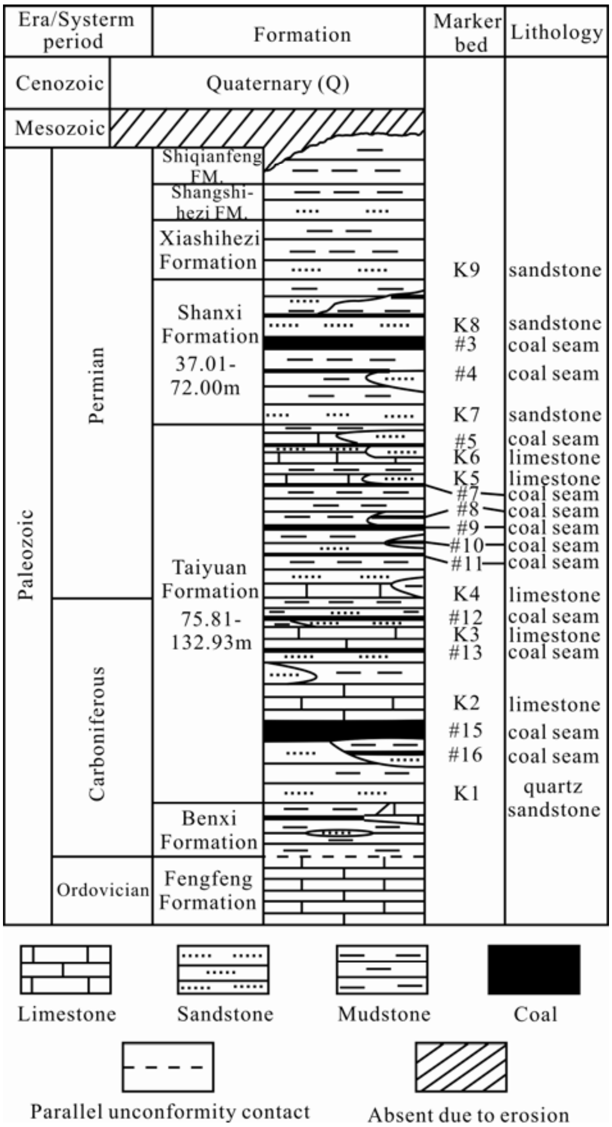

Fig. 2. Delineation of the stratigraphic characteristics in SQB.

composed of medium and fine-grained sandstones, mudstone, siltstone, limestone and coal seam; the thickness of Taiyuan Formation is between 76 m to 133 m, most of which is around 100 m. The primary target coal seams of CBM exploration and exploitation in this region are No.3 coal seam of the Shanxi Formation and No.15 coal seam of the Taiyuan Formation.

No.15 coal seam is situated in the lower part of Taiyuan Formation, around 90 m away from the upper No.3 coal seam. The thickness of No.15 coal seam varies from 0.21–9.87 m, with an average of 3.26 m; this seam generally contains 3–6 mudstone or carbonaceous mudstone interbeds. The immediate roof rocks are mainly mudstone, argillaceous limestone and K2 limestone. The floor is mostly mudstone. The maximum vitrinite reflectance ($R_{o, max}$) of No.15 coal seam varies from 2.13–4.25%, with an average of 3.14%; the coal rank ranges from semianthracite to anthracite. The major maceral component of No.15 coal seam is vitrinite, with an average content of 82%; the second is inertinite, with an average content of 17.6%; the lowest is exinite, with an average content of only 0.4%. The ash yield varies from 10%–25% (mainly from 10% to 20%), indicating that this seam belongs to low-medium ash coal according to GB/T15224.2-2010.

3 Samples and Methods

3.1 Sampling and experiments

The data such as coal thickness, burial depth, gas content, well test permeability and coal roof lithology of No.15 coal seam used in this study were collected from the measurement results from 14 coal mines and 28 CBM wells.

A total of 6 fresh block samples were obtained from Gushuyuan, Fenghuangshan, Wangtaipu, Sihe, Sihe No.2 and Chengzhuang coal mines in SQB. The samples were processed into small blocks with the maximum length of 10 mm for mercury injection experiment following the national standard SY/T5346-2005. The test results are shown in Table 1.

Fifteen produced water samples were obtained directly from the discharge points of 15 under-production CBM wells (Fig. 1) which only exploit No.15 coal seam and all the wells have been working for more than 1.5 years. In addition, 2 water samples of the roof K2 limestone of No.15 coal seam were also collected in Fenghuangshan coal mine and Sihe No.2 coal mine respectively.

Conventional cation and anion in the water samples were tested in the National Key Laboratory of Environmental Geochemistry in Guiyang, China, and the test results are shown in Table 2. Meanwhile, isotopic analyses were obtained from the same laboratory as well. Stable isotopes of water (deuterium, D, and oxygen,^{18}O) are reported in delta notation (δ) in per mile (‰) relative to known standards (VSMOW, Vienna Standard Mean Ocean Water for D and ^{18}O).

Moreover, the results of hydrogen and oxygen stable isotopes analyses of 12 water samples collected from this area and tested by Wang Shanbo et al. (2013) were applied for reference, and the isotopic analyses method of the reference is the same as the method used in this paper. Among these 12 samples, 11 samples are from K2 limestone, including 2 samples from Wangtaipu coal mine, 4 from Sihe No.2 coal mine and 5from Gushuyuan coal mine; another one is from No.15 coal seam in Wangtaipu coal mine.

3.2 AHP model for predicting CBM production potentials

Analytic hierarchy process (AHP) is a comprehensive analysis method that incorporates quantitative and qualitative analysis, and it can help decision-makers to rank multiple-attributes of parameters by deriving priorities (Satty, 1990). AHP can systematically decompose a complex problem into several evaluation levels or criteria (Harker and Vargas, 1987). The detailed principles and processes for AHP model, including the evaluation of parameters, mathematical methods and uncertainties can be found in Yao et al. (2008a).

A three-level AHP evaluation model was used in this work for predicting the CBM potentials of No.15 coal seam in the SQB (Fig. 3). The goal of AHP evaluation model is to identify a comprehensive evaluation score U called favorability index with values from 0–1.0. The value of U in the first level determines the degree of favorableness for CBM production potential, and the higher U value would obtain the more favorable CBM production potential. The second level represents the three different types of evaluation-criteria: the resources potential (U_1) with a weight of 0.2, the exploitation potential (U_2) with a weight of 0.5 and the hydrogeological condition (U_3) with a weight of 0.3. These three criteria are decomposed into eight technically alternative parameters (sub-criteria). The weights used here represent the index of importance of the criteria for evaluating the score of U. Higher weight values mean more significant evaluation results. All weights in the current hierarchy in the AHP model (Fig. 3) are assigned based on two respects: (1) the judgment and experience of geologists; (2) influencing degree affecting the CBM productivity of No.15 coal seam discussed in the part 5. The evaluated model established in the paper was aimed at the No.15 coal seam in SQB, and may be no longer applicative in other CBM areas. Modeling calculation is fulfilled using the software "MapInfo professional 8.5" in a Geographic Information System (GIS). Results of every evaluation parameter (e.g., permeability, coal thickness

Table 1 Test results of mercury injection experiment for the coal samples from SQB

Sample no.	Coal mine	Coal seam	Porosity (%)	Specific surface area (m^2/g)	Pore volume (mL/g)	Percentage of pore volume (%)			
						Micropore (<10 nm)	Transitional pore (10–100 nm)	Mesopore (100–1000 nm)	Macropore (>1000 nm)
GSY-1	Gushuyuan	15	4.54	18.962	0.0355	57.18	24.23	2.82	15.77
FHS-1	Fenghuangshan	15	5.55	24.530	0.0451	58.31	25.94	3.77	11.97
WTP-1	Wangtaipu	15	3.72	13.828	0.0251	58.57	26.29	3.59	11.55
SH2-1	Shihe No.2	15	6.23	23.492	0.0487	50.72	28.34	4.93	16.02
SH-1	Shihe	15	4.81	20.681	0.0379	58.58	25.07	3.17	13.19
CZ-1	Chengzhuang	15	4.68	20.680	0.0367	60.49	28.61	4.36	6.54

Table 2 Composition of Water Samples Collected from SQB

Well no.	δD (‰)	δ^{18}O (‰)	TDS (mg/L)	Ion concentration (mg/L)					
				K^++Na^+	Ca^{2+}	Mg^{2+}	Cl^-	SO_4^{2-}	HCO_3^-
T-4	−81.25	−10.93	882.46	308.69	5.49	6.33	93.09	0.25	923.25
T-24	−81.43	−11.00	917.83	277.86	4.69	1.80	82.21	0.62	1088.56
Z-37	−74.37	−10.27	1630.52	742.36	2.76	10.23	441.93	21.45	809.15
Z-39	−78.19	−10.85	1365.68	589.88	7.17	5.42	97.67	0.41	1316.75
Z-70	−74.73	−10.09	1280.24	525.90	1.24	5.67	210.41	0.77	1053.80
Z-7	−77.00	−10.38	1022.85	383.49	8.21	4.51	118.23	0.52	998.99
Z-76	−76.67	−10.59	1128.50	472.45	5.73	3.45	152.08	0.54	974.03
Z-86	−76.64	−10.61	1091.39	421.61	5.99	4.78	128.78	1.51	1042.60
H-14	−82.84	−11.33	2863.84	635.69	118.21	79.83	238.56	1175.81	1223.60
C-71	−75.22	−9.89	1213.00	369.91	12.96	9.41	35.84	561.56	439.16
Z-46	−76.90	−10.69	1518.06	656.32	9.00	5.73	83.50	1.71	1517.37
Z-42	−74.10	−10.49	1586.82	690.19	11.95	7.04	96.60	0.37	1557.19
Z-15	−69.11	−9.59	1802.19	795.69	1.09	3.60	92.20	6.82	1802.09
Z-17	−72.15	−10.46	1960.77	775.45	1.37	5.25	92.31	3.21	2160.53
S-1	−79.22	−11.17	2380.78	1094.61	11.40	5.54	70.77	0.16	2394.23
SH2(lim)	−67.04	−8.83	996.25	176.66	79.56	55.46	40.261	329.071	1234.42
FHS(lim)	−68.51	−9.18	1352.09	383.56	152.79	49.71	68.792	859.094	846.046

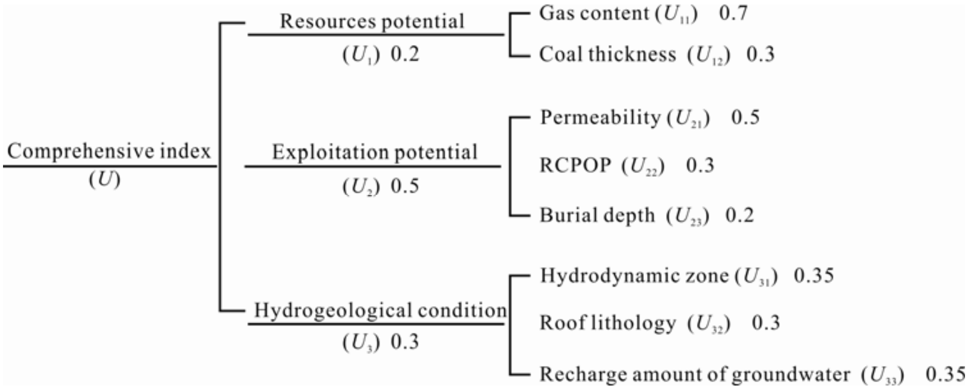

Fig. 3. The AHP evaluation model with evaluation factors and their weights.
(a), Numbers in the diagram show the weights in their current hierarchy.

and gas content) were obtained by fuzzy mathematics and vector stacking calculations in the GIS system. Finally, evaluation values for each area were synthesized to predict the high-yield potential regions for CBM production of No.15 coal seam.

4 CBM Production Characteristics of No.15 Coal Seam

The CBM wells that only exploit No. 15 coal seam in SQB are relatively rare at present. In this work, the production history data of 28 vertical wells were collected, and the wells are distributed in Zhengzhuang, Shizhuang, Fanzhuang, Panzhuang and Chengzhuang CBM Blocks, respectively. Gas and water production rates as well as their variation trends differ greatly in different production stages in CBM wells (Colmenares and Zoback, 2007; Lv et al., 2012; Tao et al., 2014). Therefore, the average gas production rate (hereafter referred to as gas rate, in m^3/d) and average water production rate (hereafter referred to as water rate, in m^3/d) for the first 600 days were calculated to analyze the temporal characteristics of the 28 vertical CBM wells. 600d was taken as a comparison standard for the following reasons: 1) the producing time of the wells is different, and the producing time of the 28 wells has all surpassed 600d; 2) it guarantees a long gas production time.

On the whole, the gas production of No.15 coal seam in SQB is lower compared with No.3 coal seam (Tao et al., 2014). According to the previous classification scheme of gas production set by Liu et al. (2013) in this area, among the 28 CBM wells (Fig. 4), there are 6 high-production rate wells (gas rate > 1000 m^3/d), 2 medium-production rate wells (500 m^3/d < gas rate < 1000 m^3/d), 7 low-production rate wells (100 m^3/d < gas rate < 500 m^3/d) and 13 drainage wells (gas rate < 100 m^3/d). Of all the 28 wells, the maximum peak gas production rate is 9836 m^3/d, and nearly half of the wells have a peak gas production rate over 1000 m^3/d, however, the high production period of most wells is short, and therefore the overall gas rate tends to be low. It can also be seen from Fig. 4 that the variation trend of the gas rates is basically in line with the peak gas production rates.

According to the gas production curve shape, the 28 CBM wells can be divided into four types (Fig. 5), namely, “increasing type” (type A), “stable type” (type B), “undulating type” (type C) and “decreasing type” (type D). The gas production curves of high-production wells (Fig. 5a) are type A and type B basically with features of higher peak gas production and longer high production period; the only two medium-production (Fig. 5b) wells belong to type C; the gas production curves of the 7 low-production wells (Fig. 5c) appear as type A, type C and type D, and among them type D is the major type with features that the gas production decreases rapidly after it reaches the peak.

5 Geological Controls over CBM Productivity

CBM productivity is affected by various factors, for instance, gas content, coal rank, coal distribution, permeability, pore and fracture structures, groundwater flow, and depositional, structural setting and so on (Kaiser et al., 1994; Yao et al., 2009a; Lv et al., 2012). In this paper, seven factors including coal thickness, burial depth, gas content, porosity, ratio of critical desorption pressure to coal reservoir pressure (RCRP), permeability and hydrogeological condition were analyzed to study their impacts on the gas productivity of No.15 coal seam in SQB. In addition, engineering factors such as hydraulic fracturing and completion techniques also affect the gas productivity of CBM wells (Johnson et al., 2002; Tao et al., 2014), however, due to the lack of related data, they are not discussed in this study.

5.1 Coal thickness

Coal is a reservoir and trap for coalbed methane (Bustin

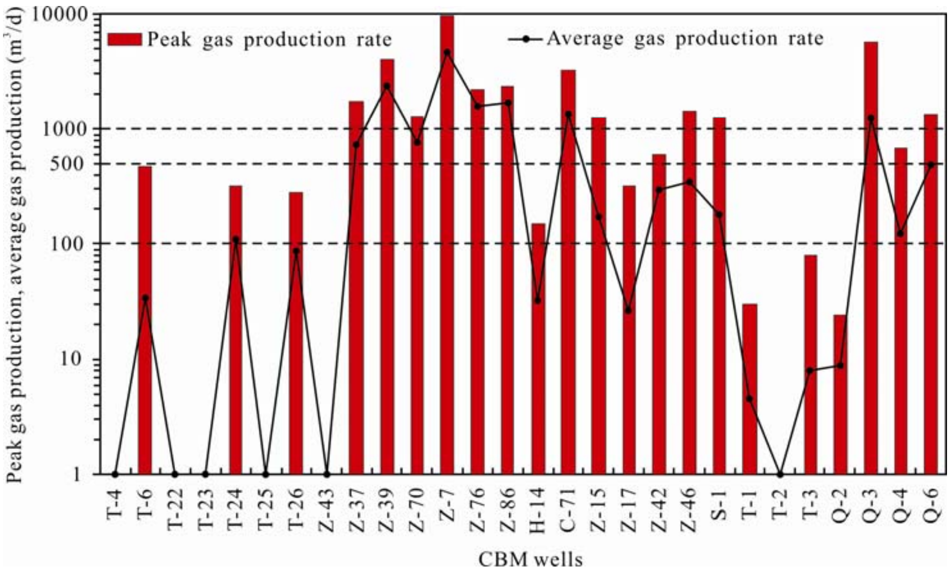

Fig. 4. CBM Productivity of No.15 coal reservoir in SQB.

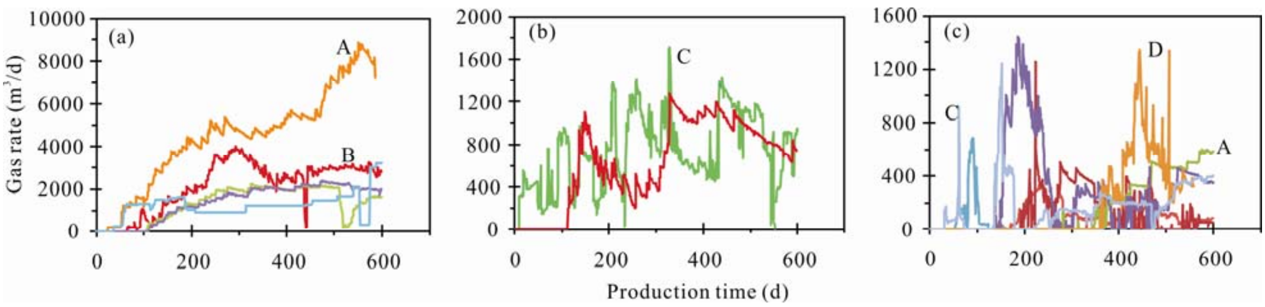

Fig. 5. Gas production curve types of various productivity CBM wells in SQB.
(a), High-production rate wells (a-A: increasing type; a-B: stable type); (b), Medium-production rate wells (b-C: undulating type); (c), Low-production rate wells (c-A: increasing type; c-C: undulating type; c-D: decreasing type).

and Clarkson, 1998), and a prerequisite for CBM production as well (Pashin, 1997). Theoretically, in the same geologic setting, the thicker the coal thickness is, the more abundant the gas resources inside the seam are, and the higher the gas production of the well is. However, the relationship between coal thickness and gas production capacity seems more complex in practice. Lv et al. (2012) found that the occurrence of thick coal seams leads to poor gas productivity of No.3 coal seam in Fanzhuang block possibly because it increases the vertical heterogeneity of coal and reduces the depressurization efficiency during the initial water pumping period. Pashin (1997) put forward that the perforated coal thickness has a poor correlation with gas production. While, most scholars still held that gas production has a positive correlation with coal thickness (Yao et al., 2009a; Zhang Peihe et al., 2011; Liu et al., 2012; Meng et al., 2014).

For the No.15 coal seam in SQB, except one abnormal point within the dotted ellipse, the coal thickness presents a poorly positive correlation with the average gas production (Fig. 6), and it seems that the occurrence of a thick coal seam tends to result in good CBM production.

5.2 Burial depth

The influence of burial depth on CBM development has two sides: on the one hand, the gas content rises with the increase of burial depth in the study area, which is beneficial to the CBM exploitation (Fig. 7a); on the other hand, with the increase of the burial depth, the crustal stress increases and the permeability of the coal seam gradually decreases (Mckee et al., 1998; Fu Xuehai et al., 2001) (Fig.7b), which leads to growing difficulty in the depressurization of coal reservoir and the seepage of CBM into the wellbore. The burial depth of No.15 coal seam in SQB varies from 81.84 m to 1423.82 m. Fig. 8 shows that the gas rate first increases and then decreases with the increasing depth as a whole, and the turning depth is approximately between 650 and 700 m. And that illustrates that: above the turning depth, with the increase of the burial depth, the positive effect of the increase of gas content on CBM production is greater than the negative effect of permeability reduction on CBM production; while below the turning depth, the negative effect of permeability reduction is greater than the positive effect of the increase of gas content. It should be noted that the relatively poor correlation between burial depth and gas rate is possibly because of other factors' joint influence. From Fig. 8 it can also be seen that the burial depth of high-production rate wells is between 550 to 950m; the only two CBM wells with the gas rate over 2000 m^3/d have the burial depth of less than 650 m; when the burial depth is over 1000 m, the CBM production is worse.

Fig. 9 shows that the burial depth of coal seam No.15 in the east side of Sitou Fault System is below 800m, and all the high-production rate wells are located in this area (Fig. 8). However, the burial depth in the area of Zhengzhuang and North Zhaozhuang is greater than 1000m, and it is difficult for CBM wells to achieve the desired production using the existing technology in China.

5.3 Gas content

Gas content, which influences the CBM producibility (Scott, 2002), is one of the most important factors for CBM exploration and development. In the same structural setting, a high gas content means a high gas saturation and a short gas breakthrough time (Lv et al., 2012; Tao et al., 2014). According to 116 gas content test data obtained from CBM parameter wells and production-test wells, the gas content of No.15 coal seam in SQB ranges from 0.49 to 36.80 m^3/t (dry ash-free basis, the same below), with an average up to 20.52 m^3/t. Fig. 10 shows that the correlation between the average gas rate and gas content is poor, and the data points are discrete. If the gas content is lower than 15 m^3/t, the gas rate of wells is less than 200 m^3/d; the gas content of medium and high production rate

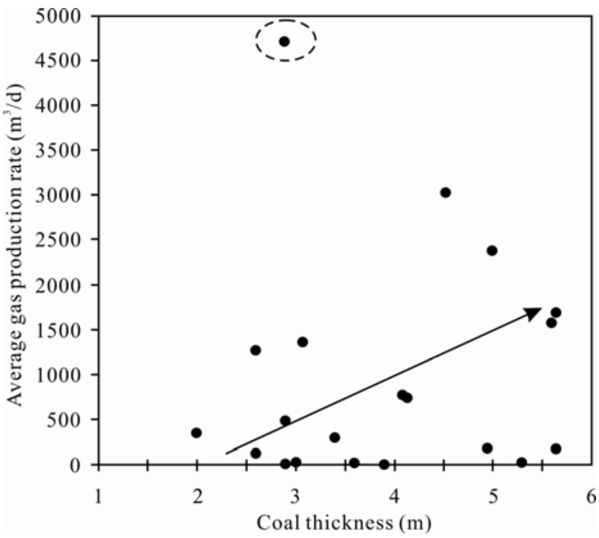

Fig. 6. Scatter plot of gas rate and thickness of No.15 coal seam in SQB.

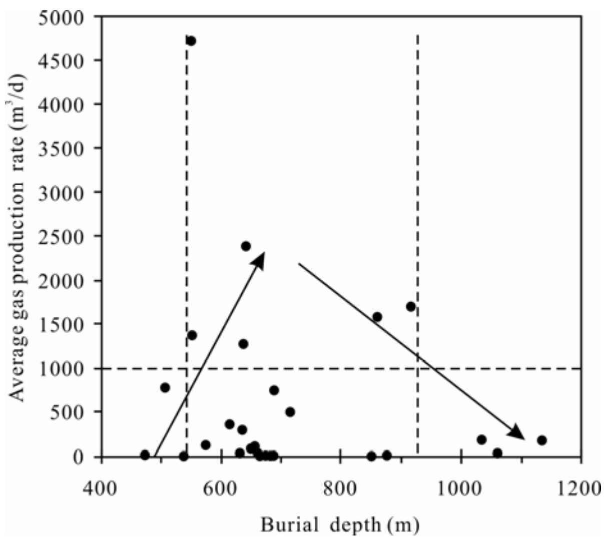

Fig. 8. Scatter plot of gas rate and burial depth of No.15 coal seam in SQB.

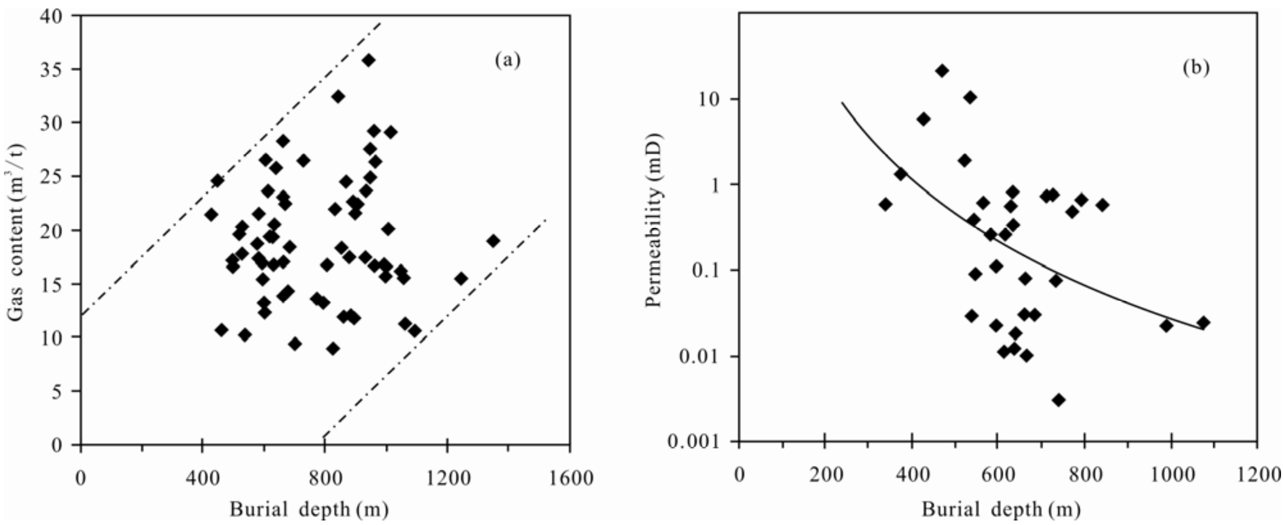

Fig. 7. Relationship between burial depth and gas content (a) and permeability (b) of No.15 coal seam in SQB.

wells is mainly between 15 to 26 m^3/t (the points within the square with dotted lines), however, the gas content of most low gas production rate and drainage wells is also in this interval (the points within the square with solid lines), besides, the two wells (Fig. 10) with the highest gas content which is more than 30 m^3/t don't acquire the expectative gas production as well. Thus, it is inferred that gas content may not be the decisive geological controlling factor impacting the gas production of No.15 coal seam in this study area, so some other factors such as permeability, porosity and pore structure, and hydrogeological condition must be considered.

The combination of Fig. 9 and Fig. 11 shows that CBM wells with high gas content and shallow burial depth usually have a good production. For example, in Panzhuang area the gas content is high and the burial depth is relatively shallow, and the gas production of the wells is good possibly because of high permeability; in Zhengzhuang area, the gas content is also high, but the burial depth is deep, which leads to a low permeability, thus, the gas production of the wells is poor. In the north of the study area, the gas content is lower and the burial depth is deeper, leading to difficulty in acquiring a high yield for the CBM wells. The gas content in Shizhuang area is higher than 20 m^3/t, and the burial depth is less than 800 m, however, the gas production of the wells is the worst; therefore, it is speculated there must exist other crucial geological controlling factors.

5.4 Ratio of critical desorption pressure to original coal reservoir pressure (RCPOP)

The critical desorption pressure (CDP) is the

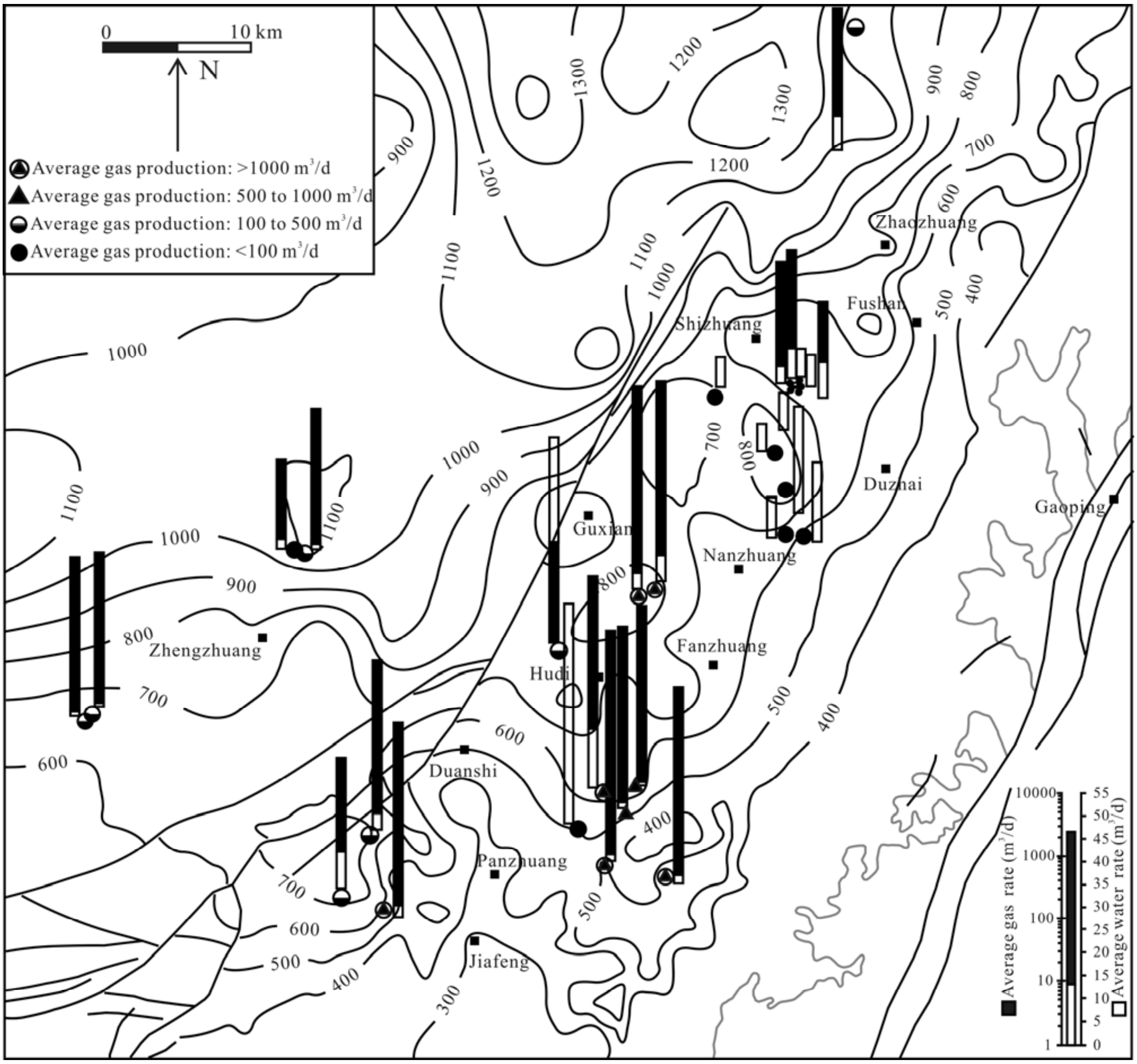

Fig. 9. Spatial distribution of gas rate and burial depth of the No. 15 coal seam in SQB.

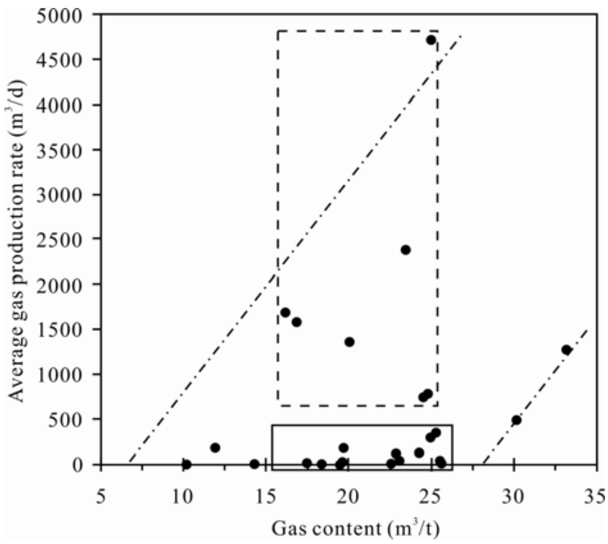

Fig. 10. Scatter plot of gas rate and gas content of No.15 coal seam in SQB.

corresponding reservoir pressure when the equilibrium between CBM adsorption and desorption is achieved at the original formation conditions. On the isothermal adsorption curve, CDP is the reservoir pressure that corresponds to the initial measured gas content. Theoretically, the greater of RCPOR is, the closer the CDP to the original reservoir pressure (OPR) is, and the easier and earlier of CBM desorption will be, and the better of gas production will be. Moreover, a high RCPOR means a shorter time of single-phase water flow stage that the CBM well would undergo, which is beneficial to reduce the permeability damage caused by the effective stress during the depressurization stage (Walsh, 1981; Yao et al., 2009b). Fig. 12 shows that the gas rate has a positive correlation with RCPOR. The RCPOR of well Z-39 and well Z-7 is higher than 0.9 which is close to saturation condition, and the gas production is high and high-production period is longer; while the wells of which

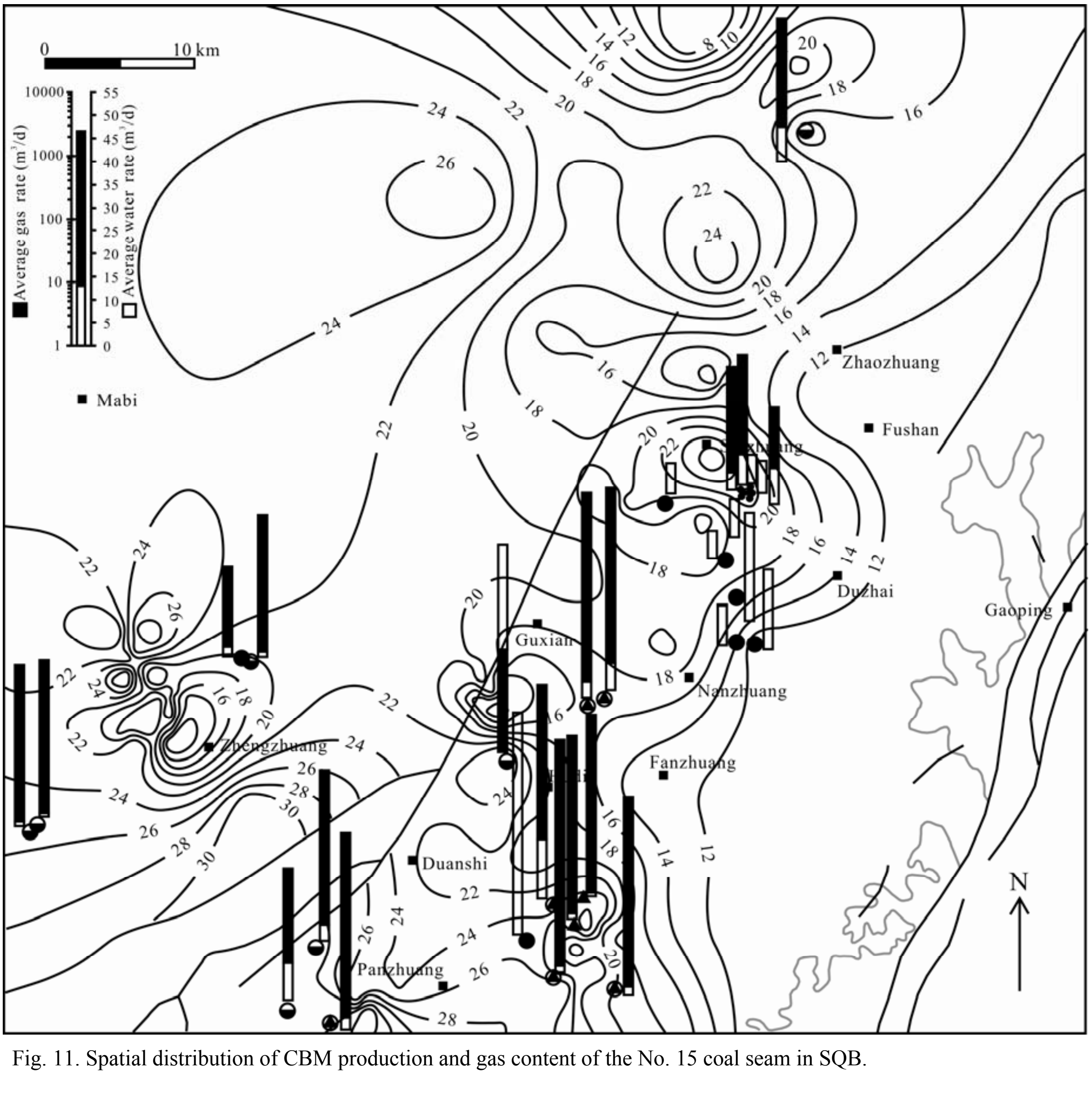

Fig. 11. Spatial distribution of CBM production and gas content of the No. 15 coal seam in SQB.

the RCPOR is lower than 0.55 all have a bad gas production.

According to the 42 isothermal adsorption test data of coal samples from drilling, the RCPOR of No.15 coal seam in SQB varies from 0.14–1.75 (avg. 0.53). In the region, the RCPOR gradually increased from north to south as a whole (Fig. 13), and it differs significantly among different CBM blocks. In Panzhuang area, the wells have the highest RCPOR, and the RCPOR of all 5 wells in this block is higher than 1, but the gas production of two of them is bad possibly because of other geological or engineering factors' impact. The RCPOR of Fanzhuang area ranges from 0.5–0.8, the south of Shizhuang from 0.16–0.88 (avg. 0.42) and the north of Shizhuang from 0.05–0.72 (avg. 0.32). In Zhengzhuang area, the average RCPOR is 0.31.

5.5 Porosity

The results of mercury injection experiment show that the effective porosity of the coal samples from the No.15 coal seam in SQB is from 3.72–6.23% (avg. 4.92%), revealing that this seam is a typical low porosity reservoir (Table 1) which is unfavorable for migration of CBM. As shown in Table 1, micropore (<10 nm) and transitional pore (10–100 nm) are the dominating pore types in this seam and contribute 79.06–89.10% (avg. 83.72%) of the total pore volume; while mesopore (100–1000 nm) and macropore (>1000 nm) are rare and they only contribute 10.90%–20.95% (avg. 16.28%) of the total pore volume. It is a typical characteristic of high rank coals that micropore and transitional pore (diffusion and adsorption pore, Yao et al., 2008b) providing storage space for CBM are dominant in the total pore volume; while the mesopore and macropore (seepage pore, Yao et al., 2009b) providing seepage path for CBM are poorly developed. Thus, for the high rank coals, the capacity that adsorbs the CBM is usually excellent (Zhang et al., 2018); however, the migration and output of CBM in these coal reservoirs are rather difficult (Fu et al., 2017; Li et al., 2017). Therefore, the low porosity and its pore size distribution of No.15 coals have a strong negative impact on the gas productivity of this seam.

5.6 Permeability

The permeability of coal reservoir is a crucial parameter that reflects the coal's ability of allowing the fluid to pass, and it determines the migration velocity and output efficiency of CBM (Fu et al., 2009). Many production practices and researches revealed that permeability is one of the most important reservoir parameters affecting the production of CBM (Durucan and Edwards, 1986; Moore, 2012; Tao et al., 2014; Fang huihuang et al., 2017). According to the injection/fall-off well test results obtained from 40 CBM parameter wells (Fig. 14), the permeability of coal seam No.15 varies from 0.001 to 22.12 mD in SQB, with an average of 0.90 mD, significantly lower than the permeability of the coal reservoirs in San Juan Basin (5–60 mD) and Powder River Basin (1–10 mD) (Pratt et al., 1999; Ayers, 2002).

Because coal reservoir heterogeneity is remarkable in the study area, it is difficult to discuss the relation between gas productivity and permeability through the contour map. In this work, based on the distribution of permeability testing wells and CBM producing wells, the study area were by and large divided into 5 subareas named as A, B, C, D, E, which are as shown in Fig. 14. The average permeability (AP) and gas rate of each subarea were calculated, and the results are shown in Table 3. Fig. 15 shows that the gas rate presents an obviously positive correlativity with the average permeability of each area, illustrating that reservoir permeability is a key factor that affects the gas productivity of No.15 coal seam in SQB. The permeability of coal reservoirs in area A and area E is the lowest, and the gas production is the worst; therefore, stimulating and strengthening the reservoir permeability by fracturing is an important measure to improve the gas production in these two areas.

5.7 Hydrogeological condition

Extraction of CBM is achieved by removing some of the formation aquifer water to lower the reservoir pressure of coal, forming a pressure drop funnel in a zone around the bottom of the well, and thus the CBM can desorbs from the surface of the coal matrix blocks once the pressure decreases to the critical desorption pressure (Kaiser and Ayers, 1994; Mcbeth et al., 2003). The hydrological condition not only plays an important role in the processes of CBM enrichment and preservation, but also controls the water and gas production rate during the CBM recovery, thus, it is regarded as one of the key factors in the exploration and development of CBM (Kaiser and Ayers, 1994; Scott, 2002; Pashin, 2007; Tao et al., 2014; Yao et al., 2014; Wang et al., 2015; Zhang et al., 2016). In this work, the influence of hydrological condition on CBM production was analyzed based on the discussions of the following four aspects: hydrogeochemistry, roof lithology and its distribution, hydrodynamic field of groundwater, and recharge rate of

Table 3 Statistical results of the permeability and gas production of different subareas

Subarea	A	B	C	D	E
Average permeability (AP, mD)	0.18	0.40	2.39	0.57	0.26
Average gas production (AGP, m^3/d)	212.35	628.00	1664.15	1100.12	35.38

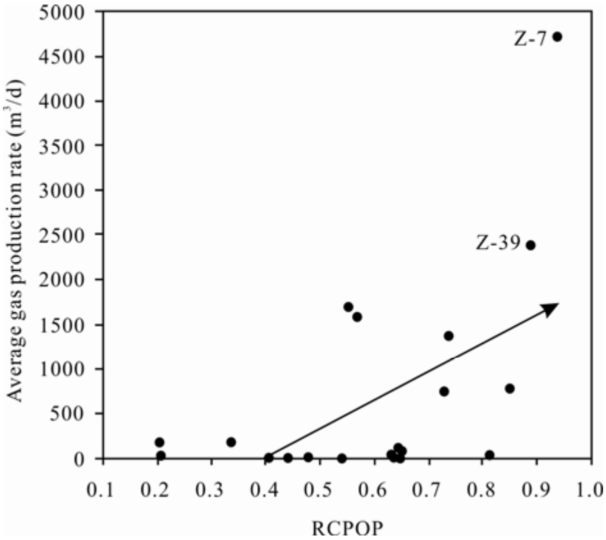

Fig. 12. Plot of gas production to RCROP of No.15 coal seam in SQB.

groundwater.

5.7.1 Composition of δD and δ^{18}O

The δD and δ^{18}O values of water have been used widely in sedimentary basins to determine the evolution and origin of the basin water (Kharaka and Carothers, 1986; Rice, 2003; Li et al., 2015; Zhang et al., 2015). As shown in Table 2, the δD value of produced water from CBM wells exploiting coal seam No.15 varies from −69.11‰ to −81.30‰ (avg. −76.95‰); the δ^{18}O value varies from −9.59‰ to −11.25‰ (avg. −10.60‰). Combining the data in Table 2 and in the reference (Wang Shanbo et al., 2013), the δD value of water from roof K2 limestone of No.15 coal seam ranges from −63.90‰ to −83.10‰ (avg. −71.76‰); the δ^{18}O value ranges from −7.30‰ to −10.90‰ (avg. −9.21‰). The δD value of water from coal seam No.15 in Wangtaipu coal mine is −85.40‰, and the δ^{18}O value is −11.00‰.

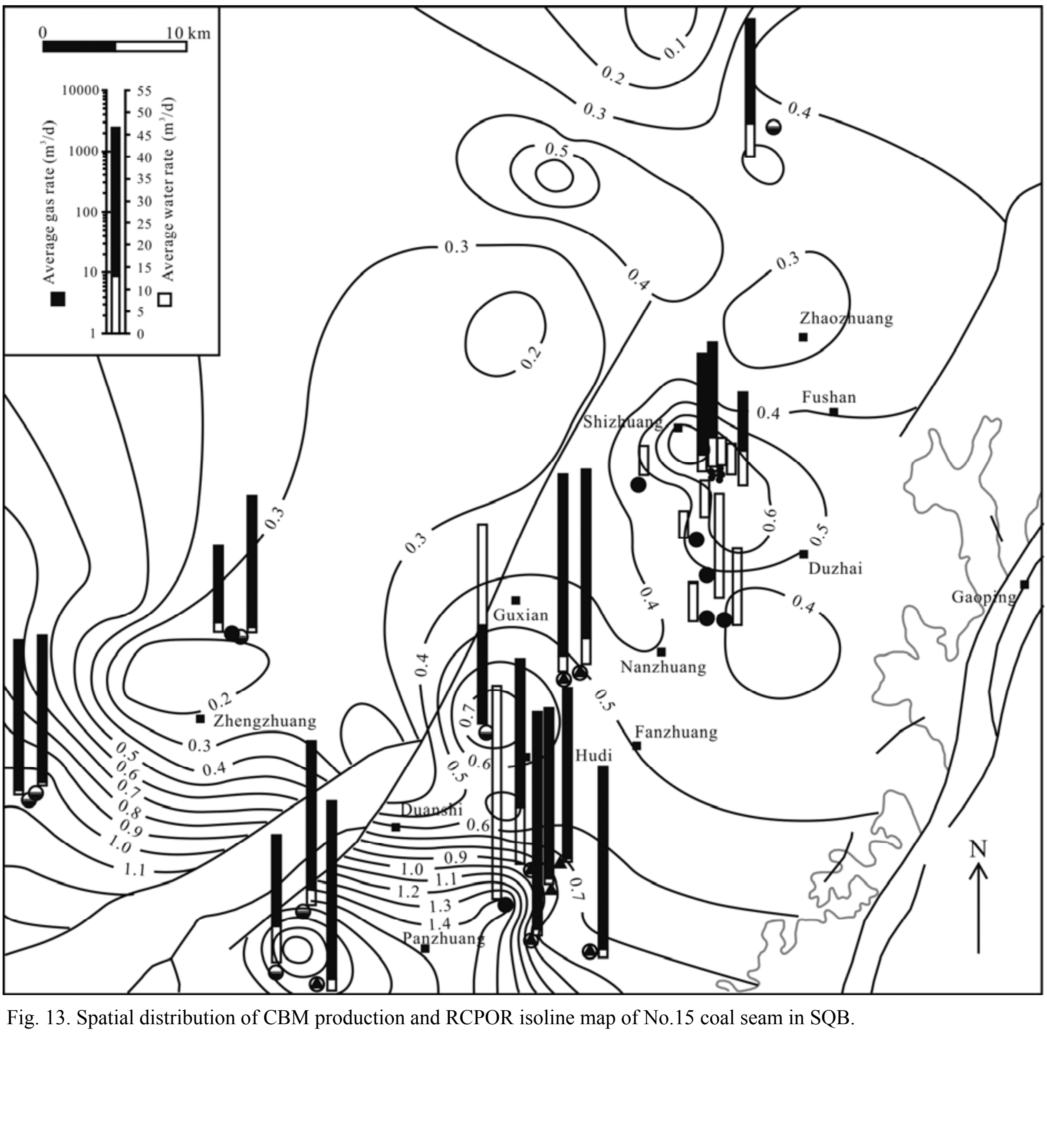

Fig. 13. Spatial distribution of CBM production and RCPOR isoline map of No.15 coal seam in SQB.

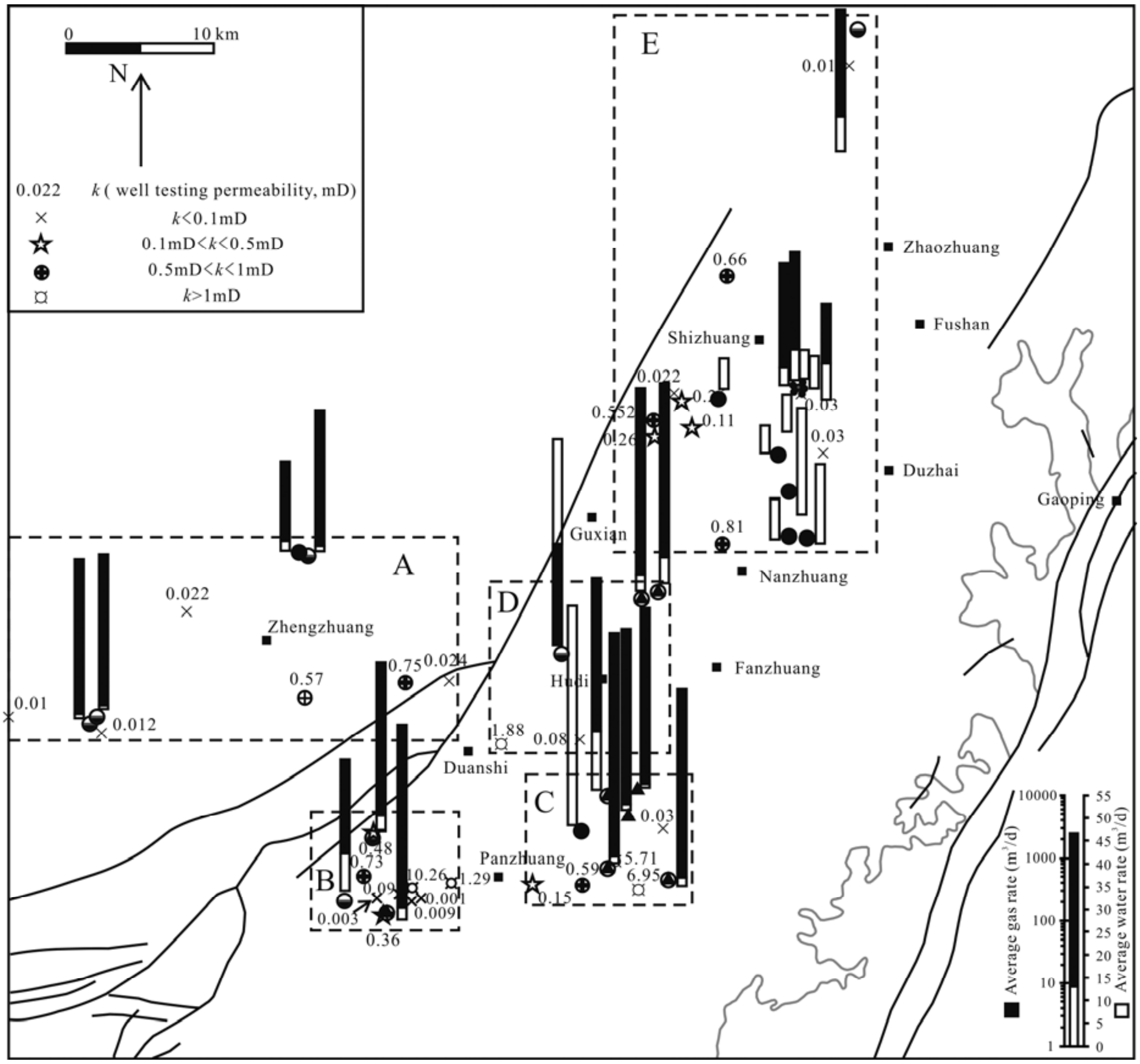

Fig. 14. Spatial distribution of CBM production and permeability of the No.15 coal seam in SQB.

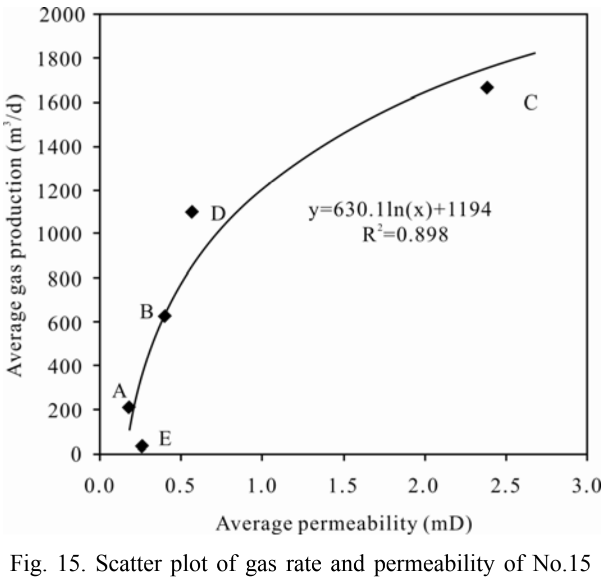

Fig. 15. Scatter plot of gas rate and permeability of No.15 coal seam in SQB.

The δD and δ^{18}O values of water samples are compared with the local meteoric water line (LMWL, function (1)) and the local evaporation line of surface water (LEL, function (2)) defined respectively by Liu jinda et al. (1997) and Zhang et al. (2015):

$$\delta D=7.01\delta^{18}O+0.11 \tag{1}$$

$$\delta D=2.67\delta^{18}O-51.63 \tag{2}$$

Specifically, due to the lack of monitoring δD and δ^{18}O values of atmospheric precipitation in Jincheng area or Qin River, the LMWL (Fig. 16) used in this work was based on the monitoring data from Zhengzhou (Fig. 1a), the nearest city to our study area in China's monitoring network for atmospheric precipitation isotope.

It can be seen that the composition of δD and δ^{18}O of almost all the water samples are situated between the LMWL and the LEL or around them (Fig. 16), indicating that the initial source of them is meteoric water. In addition, the composition of δD and δ^{18}O of produced

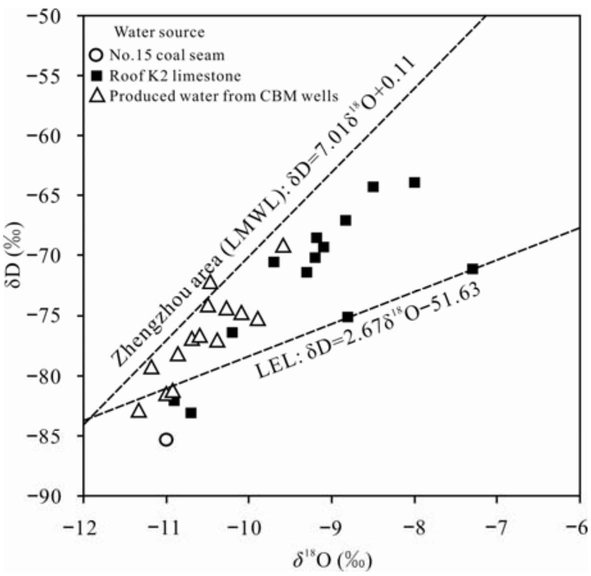

Fig. 16. Isotopic composition of δD and δ^{18}O of collected water samples in SQB.

water from CBM wells are heavier than that of the water from coal seam No.15, and lighter than that of the water from K2 limestone, illustrating that the produced water of CBM wells is the mixed water of K2 limestone water and No.15 coal seam water. Moreover, isotopic composition of the produced water of some CBM wells is even close to that of K2 limestone water, implying that K2 limestone water may be the major source of the produced water for these wells. Therefore, supply intensity of K2 limestone water directly affects the difficulty degree in drainage and depressurization of No.15 coal seam.

Meteoric water interacts with the rock and constantly dissolves the soluble mineral components in the rock while it flows underground, meanwhile, the dissolved mineral components containing hydrogen and oxygen continually react isotope exchange with groundwater, leading to constant changes of δD and δ^{18}O. Previous researches show that the deuterium values will increase with groundwater flowing (Li et al., 2015) and were associated with the total dissolved solids (TDS) (Rice, 2003). In this study, it was found that strong positive correlation exists between the deuterium values and TDS except one abnormal point within the dotted ellipse (Fig.17). Wang et al. (2015) deemed that in the area with lighter deuterium value in the groundwater, the water-rock interaction is intense, and the water alternate action is strong and the permeability of the aquifer is high. Fig. 18 shows that the water rates of CBM wells increase with the decrease of δD values, also implying that the fractures of roof K2 limestone in the area with light δD may be well developed, and the water supply to the coal seam is strong, which will bring difficulty in depressurization and thus influence the gas production.

5.7.2 Total dissolved solids (TDS) and hydrodynamic field of groundwater

In the Qinshui Basin, the depth of aquifer gradually increases from the wing to the axis, and the runoff intensity of groundwater changes from active to stagnant, and obvious hydrodynamic zonation exists in the plane (Wang Hongyan et al., 2001). The groundwater within different hydrodynamic zoning possesses different TDS characteristics and has differences in the control of CBM enrichment and production. Fig. 19a shows that the average gas production presents a two-stage change with the increase of TDS of produced water from CBM wells. When the TDS is lower than 1000 mg/L, the gas

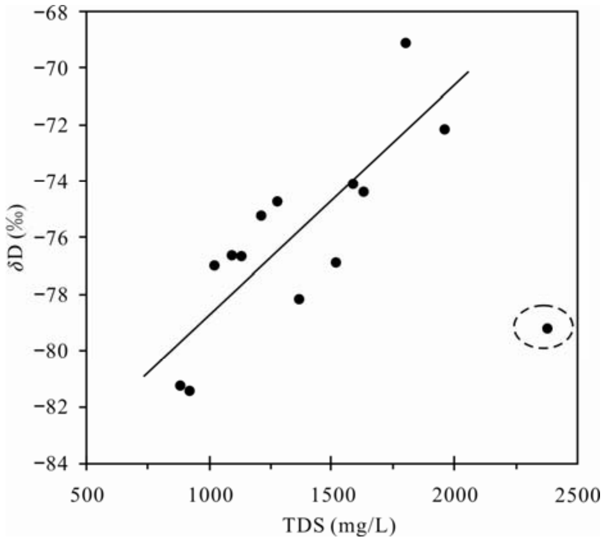

Fig. 17. Plot of δD to TDS of produced water from CBM wells in SQB.

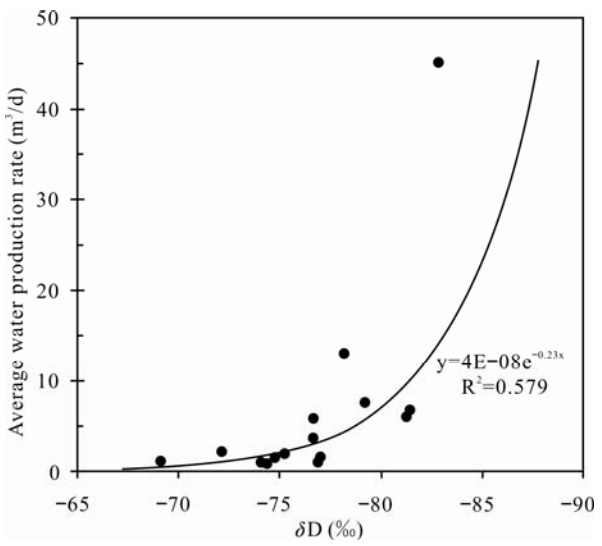

Fig. 18. Scatter plot of average water production rate and δD in SQB.

production is worse, and the two CBM wells with the lowest-TDS produced water almost have no gas production. When the TDS is over 1000 mg/L, the gas production presents obviously negative correlation with the TDS. Due to good positive correlation between δD and TDS, the relationship between δD and gas rate is similar to that between TDS and gas rate, and Fig. 19b shows that when the δD is higher than 78.5‰, the gas rate decreases with the increase of δD.

In the same geologic setting, CBM wells with low TDS produced water are close to the recharge area of groundwater system, and the coal seam is in the strong runoff zone of groundwater, where the buried depth of coal seam is relatively shallow, and the groundwater is active, and the recharge of groundwater is sufficient, and the δD in groundwater is low. This leads to a lower reservoir pressure, a lower gas content of the coal seam, and a higher water rate of CBM well and in such a situation, it is usually difficult to depressurize the coal reservoir pressure and therefore, the gas production is usually low. Taking T-1 and T-2 wells in Nanzhuang area as examples, they are close to the recharge area of groundwater (Fig. 20), and the average water production rate of the two wells reaches 8.90 m^3/d and17.33 m^3/d respectively, and there is almost no gas output in the two wells.

While CBM wells with high TDS produced water are usually in the stagnant zone of groundwater (Su et al., 2005; Lv et al., 2012), where the burial depth of the coal seam is deep, and the runoff condition of groundwater is poor, and the δD in groundwater is high. Generally, the coal seam is well confined and it has a high gas content, however, accompanied with a low permeability. Therefore, the average water production rate of a CBM well is comparatively low and the gas production is not very satisfactory. With Z-15 well in Zhengzhuang area as an example, this well is located in the stagnant zone of groundwater (Fig. 20); the TDS of its produced water is up to 1802 mg/L, and the burial depth of coal seam No.15 is 1136 m. The testing permeability of this area (area A in Fig. 14) is only 0.23mD. The average gas rate of well Z-15 is only 175 m^3/d, and the average water rate is 1.17 m^3/d.

CBM wells with medium TDS produced water are usually situated in the weak runoff zone of groundwater, where the recharge conditions of groundwater are mediocre, and the permeability of coal seam is comparatively high, and the gas production is very high (Li et al. 2015). For example, Z-7 well in the northwest of Panzhuang (Fig. 20) is in the weak runoff zone of groundwater, and the TDS of its produced water is 1022.85 mg/L; the average gas rate of the well is up to 4715 m^3/d and the average water rate is only 1.50 m^3/d.

5.7.3 Roof lithology and its distribution

Based on roof lithology statistical results obtained from 710 drill holes in the study area, the plane distribution map of roof lithology of No.15 coal seam was drawn, as shown in Fig. 21. The roof rock is mainly limestone with locally distributed mudstone, argillaceous limestone and siltstone. It can be seen from Fig. 21 that the wells with medium and high gas production rate are mainly located in the area with mudstone roof. According to the statistical results: the average water rate of wells in the area where the roof rock is mudstone is 4 m^3/d (one well that has the water rate of 48.24 m^3/d has been removed); the average water rate of wells in the area where the roof rock is limestone is 6.83 m^3/d (one well that has the water rate of 45.07 m^3/d has been removed). The average gas rate of wells in the area with mudstone roof rock is 1608 m^3/d; the average gas rate of wells in the area with limestone roof rock is only 247 m^3/d. In a word, the average water rate of wells in the area where the roof rock is limestone is

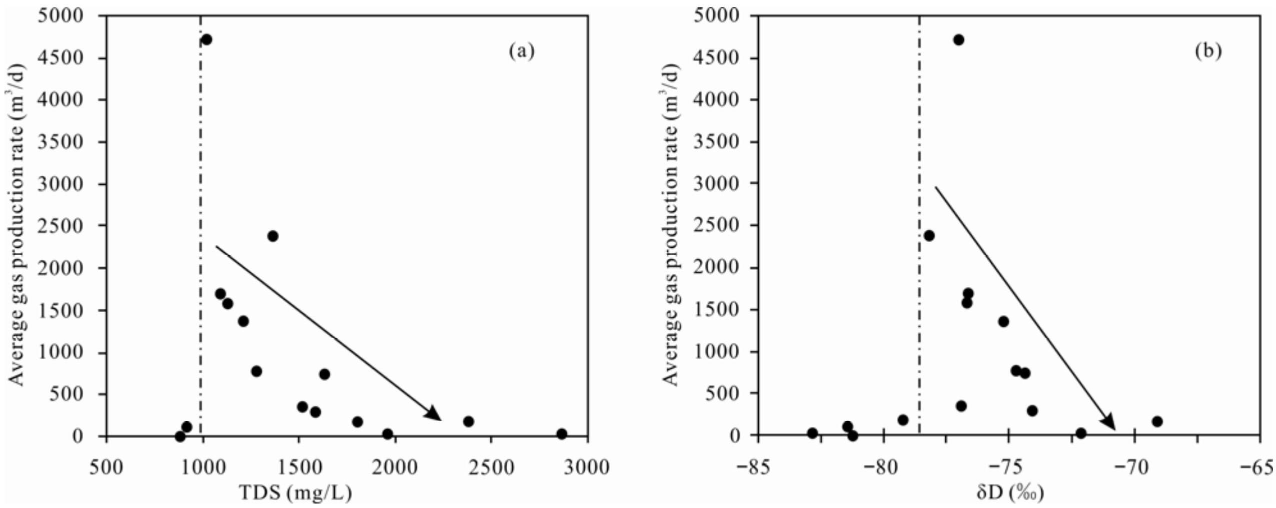

Fig. 19. Plots of gas production to TDS (a) and δD (b) of produced water from CBM wells in SQB.

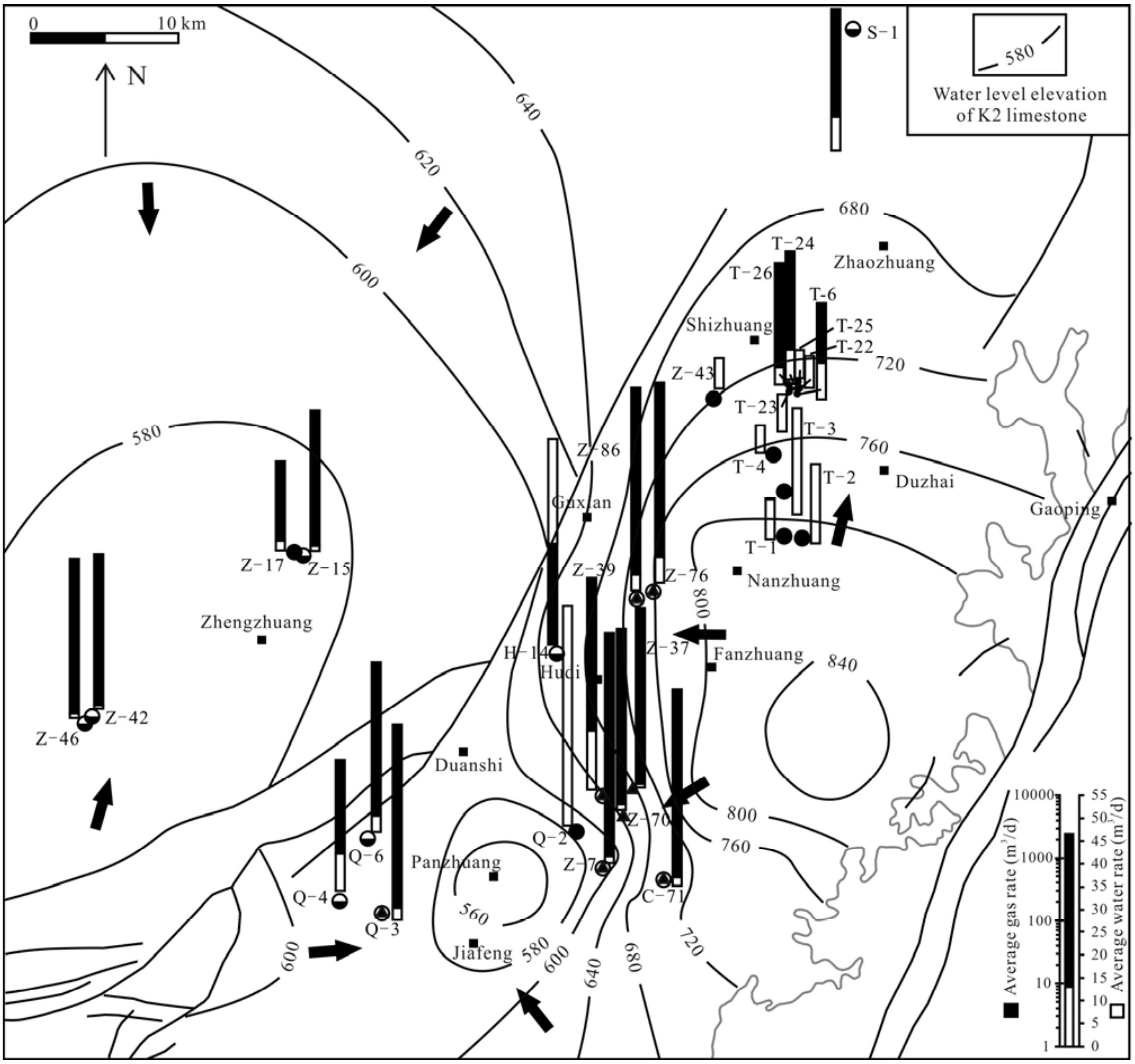

Fig. 20. The water level elevation of limestone aquifer of Taiyuan Formation in SQB.

apparently higher than that of the wells in the area where the roof rock is mudstone; however, the average gas rate declines significantly. Therefore, during the process of hydraulic fracturing operation, fracturing strength needs to be well controlled to avoid fracturing the roof limestone aquifer.

5.7.4 Recharge amount of groundwater

In the process of drainage and depressurization of coal reservoir, the groundwater can be supplied to the coal reservoir through vertical infiltration and leakage, therefore, the groundwater is the significant recharge source of gravity water of coal reservoir. The strength of groundwater recharge is directly related to the difficulty of depressurization of coal reservoir. In the same producing time, the recharge amount of groundwater to the CBM well can be measured by the average water production rate.

The average water rate of No.15 coal seam varies from 0.89–48.24 m^3/d in SQB, with an average of 8.97 m^3/d. Fig. 22a shows that the gas-water production ratio presents an obvious positive correlation with gas production, and CBM wells with higher gas-water production ratios usually have a higher gas production. In addition, CBM wells with medium and high production rates have the water rate of less than 6 m^3/d (Fig. 22b); when the water rate is over 6 m^3/d, the gas production is very low or even none.

Most of the wells between Shizhuang and Nanzhuang have the water rate over 6 m^3/d, and accordingly the gas

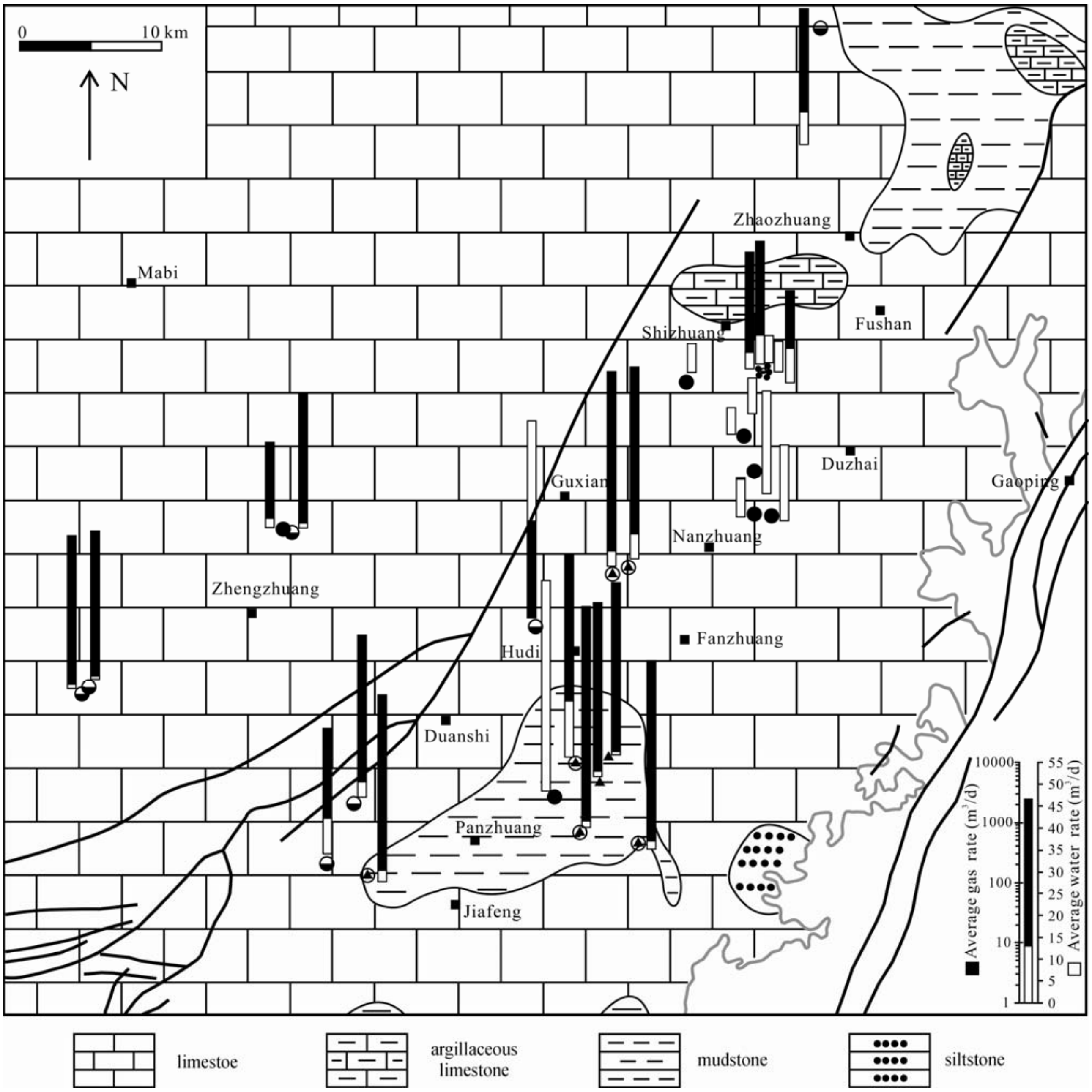

Fig. 21. Distribution map of roof lithology of No.15 coal seam in Taiyuan Formation in SQB.

rates of these wells are very low. However, a high water rate doesn't always signify a low gas production. For example, the average water rate of well Z-39 in the south of the study area reaches up to 13 m^3/d, but the average gas rate is 2381 m^3/d with a peak gas production of up to 4013 m^3/d. Besides, for well Z-76 in the north of Hudi, its average water rate is 5.8 m^3/t close to 6 m^3/t, while its average gas rate is 1578 m^3/d with a peak gas production of 2203 m^3/d. Both of the two wells have not only a high average water rate but also a high average gas rate.

Through analyzing the production history of well Z-76 (Fig. 23a), well Z-39 (Fig. 23b), and well T-24 (a representative CBM well in Shizhuang area, as shown in Fig. 23c), we can see that there are obvious differences between well T-24 and the other two wells in the water production history. For Well Z-76, the water production rate reached its peak (15.4 m^3/d) on the 107th day, and the burial depth of the fluid level varied from 253 m to 848 m during this period; after the peak water rate, the daily water production began to decrease steadily, and the fluid level remained stable basically. For Well Z-39, its water production curve shape is similar to that of Well Z-76. To be specific, the daily water production reached its peak (24 m^3/d) on the 55th day, afterwards, it began to decrease

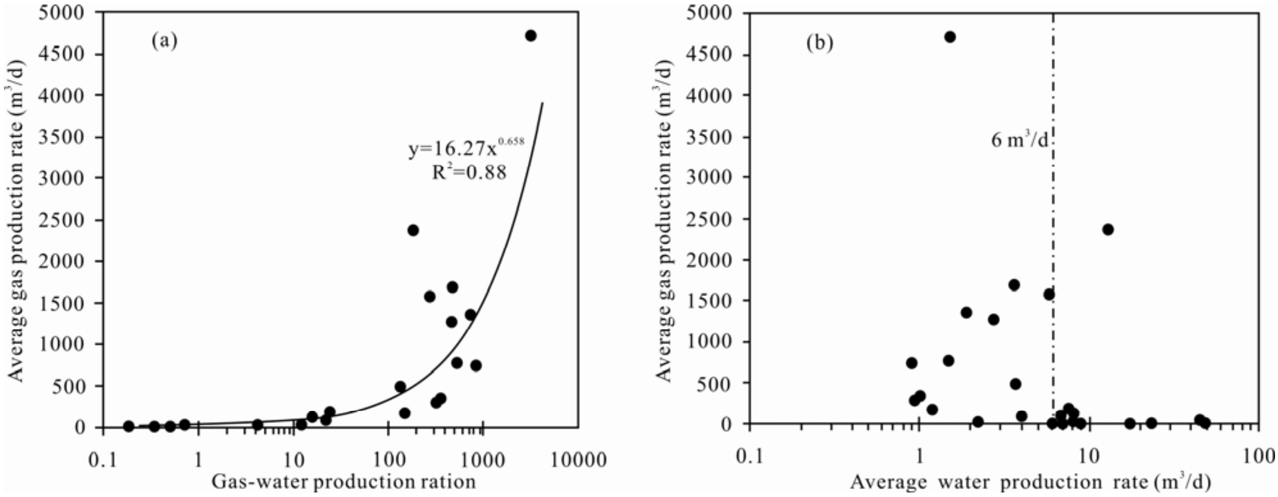

Fig. 22. Plots of gas production to gas/water ratios (a) and average water production (b) of CBM wells in SQB.

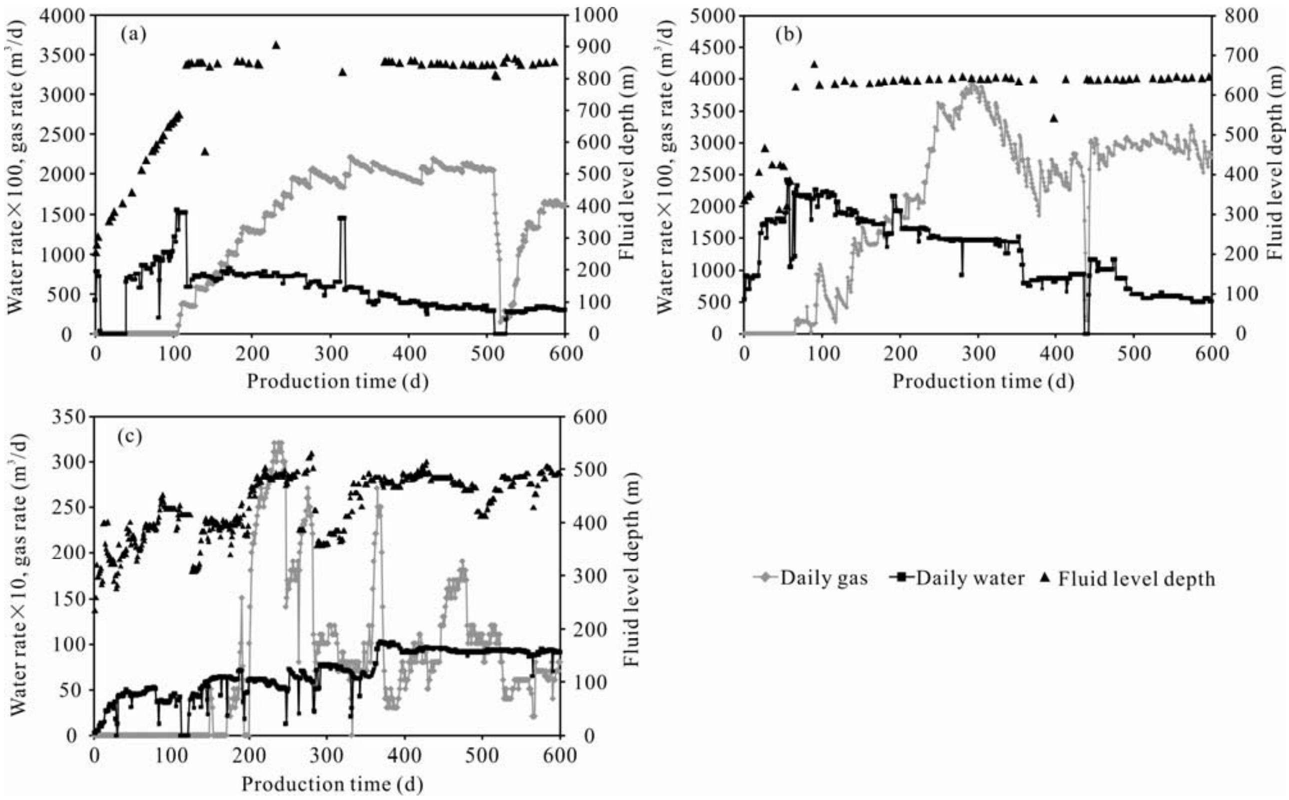

Fig. 23. Gas and water production history of representative CBM wells in SQB.
(a), Well Z-76; (b), Well Z-39; (c), Well T-24, a representative CBM well in Shizhuang area.

steadily, and the burial depth of fluid level maintained at around 63 m. While for Well T-24, the daily water production increased gradually overall, and the fluid level was extremely unstable; the daily water production on the 600th day is 9 m^3/d, and there was still no trend to decrease, that is, the water rate has not reached its peak; the average water rate is 6.74 m^3/d, which is close to that of well Z-76, but the gas rate is only 110 m^3/d. In a word, the water supply to well Z-76 and well Z-39 decreases gradually, while the groundwater maintain high-strength supply to the well T-24 unremittingly.

Furthermore, it can be seen from the hydrogeochemical analysis results of well T-24 (Table 2) that the values of δD and TDS of produced water from this well is very low. Therefore, it is speculated that for well T-24, there exists a strong hydraulic connection between No.15 coal seam and its roof K2 limestone aquifer, resulting in the water production staying at a high rate for a long time. Zou et al.

(2011) defined the coal reservoir like well T-24 as a "water pressure type reservoir". Coal reservoir of this type is in an open groundwater system. The water rate is usually high, and it is difficult to drop the formation pressure and therefore the depressurized area is limited, leading to a low even no gas production. While for well Z-76 and well Z-39, the water recharge from roof K2 limestone aquifer into coal seam is limited, the depressurized area can expand in the space, and thereby the desorption area is relatively large, so a high gas production was achieved. To sum up, high water rate is not always an indicator of a low gas production, and their relations depend on whether K2 limestone aquifer can continually and intensely recharge No.15 coal seam or not. The wells between Shizhuang to Nanzhuang have similar water production history with well T-24 and the gas production is overall low in this area at the present stage.

6 Prediction for CBM High-yield Potential Regions

6.1 Geological influence factors used to distinguish the target area

As discussed above, the geological influence factors on the CBM productivity of No.15 coal seam include gas content, permeability, RCPOP and so on (i.e., the evaluation parameters in the third level of the AHP model in Fig. 3). In the prediction for CBM high-yield potential regions, these influence factors are chosen first as the evaluation parameters and then the quantification method for these parameters should be determined.

The determination of the quantification method for each parameter is based on the data from fieldwork, experimental analysis and well tests, etc.. These parameters include some quantitative parameters such as coal thickness and gas content that can be rated by a linear piecewise continuous membership function and some others such as hydrodynamic zone and roof lithology that can be quantified by scoring tables (Yao et al., 2008a). The quantification process for all evaluation parameters are discussed below.

6.1.1 Gas content (U_{11})

The gas content of No.15 coal seam in SQB is relatively high with values from 0.49–36.80 m^3/t, with an average up to 20.52 m^3/t. As shown in Fig. 10, the CBM production increases with the gas content (V, unit: m^3/t) rises as a whole. And when V<15 m^3/t, the gas production is poor; when V is around 25 m^3/t, the gas content is relatively good. Therefore, the 15 and 25 m^3/t are defined as the lower-threshold and the upper-threshold of gas contents respectively in this work. Consequently the parameter of gas content can be rated and scored by Function (3).

$$U_{11}=\begin{cases}1 & V>25\\ 0.08V-1 & 15<V\le 25\\ 0.2 & V\le 15\end{cases} \tag{3}$$

6.1.2 Coal thickness (U_{12})

The coal thickness of No.15 coal seam in SQB varies from 0.21–9.87 m. As discussed in part 5.1, it seems that the occurrence of a thick coal seam tends to result in good CBM production. In this evaluation, the lower-threshold and the upper-threshold for coal thickness (M, unit: m) are set at 1 and 4 m, respectively. The parameter of coal thickness can be rated and scored by Function (4).

$$U_{12}=\begin{cases}1 & M\ge 4\\ \dfrac{4M-1}{15} & 1\le M<4\\ 0.2 & M<1\end{cases} \tag{4}$$

6.1.3 Permeability (U_{21})

The well-test results show that the permeability of No.15 coal seam in SQB varies from 0.001–22.12 mD (avg. 0.9 mD) and is generally lower than 1 mD. Based on previous research by Yao et al. (2008a), we define that the high-yield CBM wells are those with reservoir permeability higher than 1 mD, and the evaluation scores for permeability (k, unit: mD) >1 mD are defined as >0.6. The lower-threshold for permeability is set as 0.01 mD, which means the CBM wells with reservoir permeability lower than 0.01 mD are unrecoverable for CBM resources, accordingly, the evaluation score for permeability <0.01 mD is defined as 0. The upper-threshold for permeability is set at 5 mD. As a result, the parameter of permeability can be rated and scored by Function (5).

$$U_{21}=\begin{cases}1 & k>5\\ 0.1k+0.5 & 1<k\le 5\\ 0.444k+0.1556 & 0.1<k\le 1\\ 2.22k-0.0222 & 0.01<k\le 0.1\\ 0 & k\le 0.01\end{cases} \tag{5}$$

6.1.4 RCPOP (U_{22})

Based on the CBM development experience from No.3 coal seam in SQB (Chen Zhenhong et al., 2009; Tao et al., 2014) and the relationship between RCPOP and the gas production of No.15 coal seam in this paper, the lower and upper thresholds for RCPOP (p_r) are set at 0.75 and 0.55, respectively. Consequently the parameter of RCPOP can be rated and scored by Function (6).

$$U_{22}=\begin{cases}1 & p_r>0.75\\ 2.25p_r-0.6875 & 0.55<p_r\le 0.75\\ p_r & p_r\le 0.55\end{cases} \quad (6)$$

6.1.5 Burial depth (U_{23})

In SQB, most coals with a depth lower than about 200 m are situated in the weathering and oxidization zone of CBM, where the gas content is lower and the methane saturation is <80% (Song Yan et al., 2010). Therefore, the lower-threshold for burial depth is set at 200 m, and the corresponding evaluation score for burial <200 m is defined as 0. As discussed in part 5.2, the average gas production of CBM wells with a depth over 1000 m is very low in SQB, thus, the upper-threshold for burial depth is set at 1000 m. In addition, based on the CBM development experience from No.3 coal seam in SQB and the coal reservoirs in Ordos Basin (Yao et al., 2009a; Song Yan et al., 2013; Tao et al., 2014), the optimized burial depth for CBM development is between 500 and 700 m where both the gas content and permeability are relatively higher. For No.15 coal seam in SQB, when the burial depth is around 600 m, the gas production is relatively good. So the evaluation score at depth =600 m is defined as 1 in this work. Finally, the scoring function for burial depth (H, unit: 100 m) is defined in Function (7).

$$U_{23}=\begin{cases}0.2 & H>10\\ 2.20-0.2H & 6<H\le 10\\ 0.25H-0.5 & 2<H\le 6\\ 0 & H\le 2\end{cases} \quad (7)$$

6.1.6 Hydrodynamic zone (U_{31})

As discussed in part 5.7.2, the gas production of No.15 coal seam in the weak runoff zone (type II) of groundwater is the best, thus the U_{31} values for coal seam in the type II are defined as 0.6–1.0; the gas production in the strong runoff zone (type III) of groundwater is the worst, accordingly, the U_{31} values for coal seam in the type are defined as 0–0.2; the gas production in the stagnant zone (type I) is between in the type III and in the type II, and the U_{31} values for coal seam in the type I are defined as 0.2–0.6. The scoring model for hydrodynamic zone is summarized in Table 4.

6.1.7 Roof lithology (U_{32})

As mentioned in part 5.7.3, the roof lithology of No.15 coal seam in SQB mainly include limestone, mudstone, argillaceous limestone and siltstone. According to the degree of favorableness for CBM preservation, the roof of No.15 coal seam is divided into three types in this work. Type A is mudstone or argillaceous limestone, and the fractures are rarely developed in these rocks, which are favorable for CBM preservation. Type B is siltstone, in which the fractures are developed generally, and it causes that the degree of favorableness for CBM preservation of Type B is lower than type A. Type C is limestone, in which the fractures are well developed, and it is very unfavorable for CBM preservation; in addition, because of well developed fractures in Type C, the water abundance of limestone is relatively strong, which brings difficulty in depressurization of coal reservoir and thus influence the gas production of CBM well. The scoring model for each roof type is defined in Table 5.

6.1.8 Recharge amount of groundwater (U_{33})

In the same producing time, the recharge amount of groundwater to the CBM well can be measured by the average water production rate. As shown in Fig. 22b, when the water rate is over 6 m^3/d, the gas production is very low or even none; when the water rate is between 1 and 6 m^3/d, the gas production is better as a whole. The scoring model for different water production rates is defined in Table 6.

6.2 Distribution of CBM high-yield potential regions

The CBM production potential of No.15 coal seam in SQB is evaluated based on the GIS-based AHP model together with the evaluating parameters including gas content, coal thickness, permeability, RCPOP, burial depth, hydrodynamic zone, roof lithology and recharge amount of groundwater.

According to the results, the evaluation area is divided into six levels of subareas, level VI to level I with increasing comprehensive evaluation scores (Fig. 24), which is in the range from 0.26–0.92. The subarea level I with the highest evaluation scores (>0.8) is the most favorable area, and this category includes the Chengzhuang district and a small area in the northwest of Chengzhuang. The subarea level II with 0.7–0.8 evaluation scores is a relatively favorable area, and it mainly covers the Panzhuang district, the north and east

Table 4 Scoring model for different hydrodynamic zones of groundwater

Hydrodynamic zone	Stagnant zone (type I)	Weak runoff zone (type II)	Strong runoff zone (type III)
U31 value	0.2–0.6	0.6–1.0	0–0.2

Table 5 Scoring model for different types of coal roofs

Roof type	Type A	Type B	Type C
U32 value	1	0.8	0.6

Table 6 Scoring model for different water production rates

Average water rate (m^3/d)	<1	1~6	>6
U_{33} value	0.2–0.6	0.6–1.0	0–0.2

area of Chengzhuang, and partial area in the northwest of Hudi. The subarea level III with 0.6–0.7 evaluation scores is a moderately favorable area that mainly covers Hudi district, the south area of Fanzhuang, the southeast area of Guxian, the south area of Duanshi, the southwest area of Zhengzhuang, and the south area of Panzhuang. The subareas level IV, V and VI with evaluation scores lower than 0.6 are unfavorable areas for CBM development of No.15 coal seam, and it covers most areas in the west of Sitou Fault System and most areas in the north of Fanzhuang. Overall the CBM subareas become more favorable for the CBM development of No.15 coal seam from north to south. The CBM high-yield potential regions occur in the districts of Panzhuang, Chengzhuang and south of Hudi, with favorable burial depth and roof lithology, high gas content, high permeability and RCPOP, and low to medium groundwater recharge and runoff strength providing the most favorable conditions for CBM production.

It can be discovered in Fig. 24 that: 1) the medium and high production rate wells are basically situated in the subareas level I to level III with evaluation scores higher than 0.6; 2) low-production rate and drainage wells are basically located in the subareas level I to level III with evaluation scores lower than 0.6. However, it must be pointed out that uncertainties and imprecision exist in the evaluation results, for example, minority low-production rate lands on the subareas level II and level III, and individual drainage wells falls into the subarea level I. The reasons for the phenomenon may be: 1) Uncertainties in the evaluation methods and chosen geological evaluation parameters may result in imprecision; 2) due to a short time for water extraction, a number of CBM wells may not reach the peak production and are still at the drainage and depressurization stage; 3) the coal seam may be connect with an aquifer due to undiscovered minor faults or

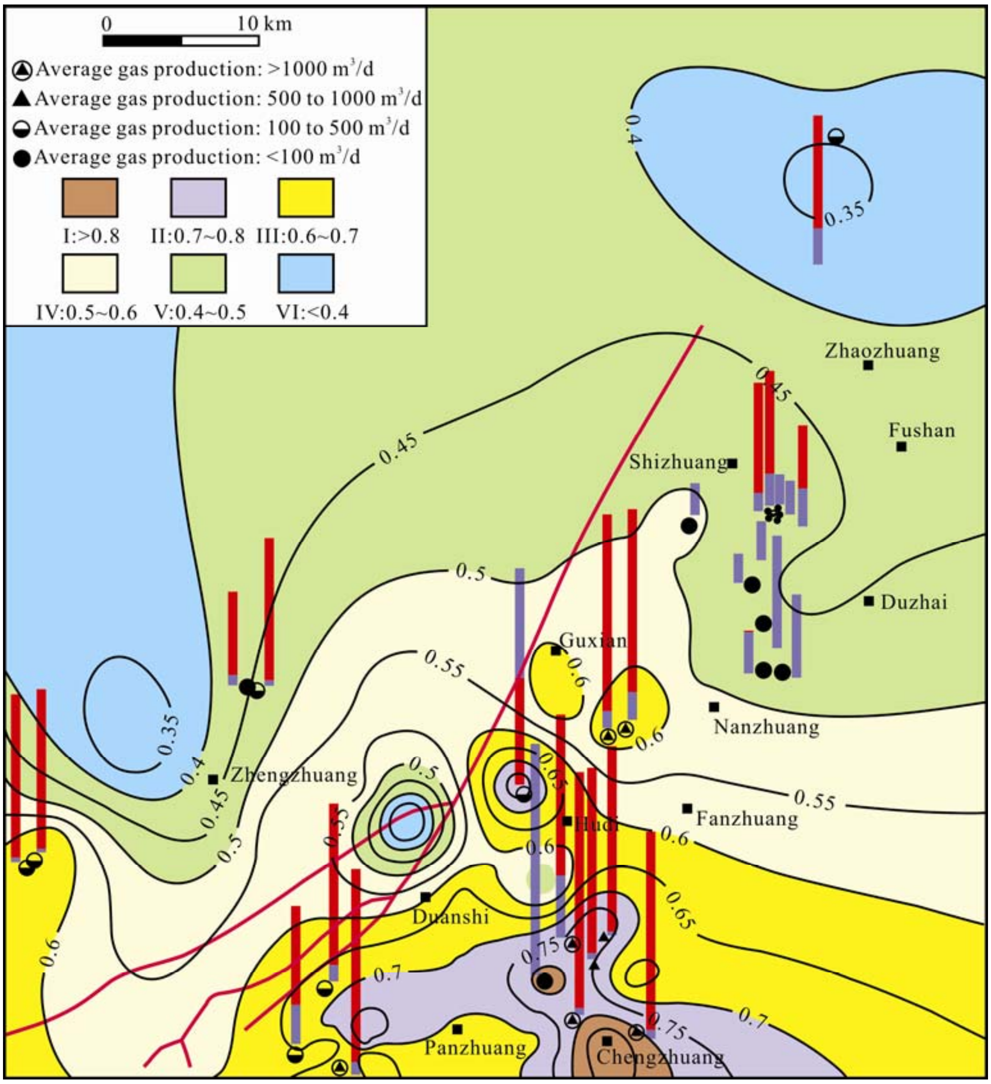

Fig. 24. The evaluation level subareas for the exploitation potential of the CBM in No.15 coal seam in Taiyuan Formation in SQB.

incorrect drilling and fracturing during well construction (Liu et al., 2012), and thus the CBM well may has a high water production rate but low gas production rate; 4) the abnormal productivity may be caused by formation damage from improper drainage. Nonetheless, the information and evaluation results presented here can provide first order guidance for the CBM development of No.15 coal seam in SQB.

7 Conclusions

No.15 coal seam in Taiyuan Formation in SQB is abundant in CBM resources and has a great potential for CBM production. Coal rank of this seam across the area ranges from semianthracite to anthracite ($R_{o,\ max}$, 2.13–4.25%, avg. 3.14%). Coal macerals are characterized by average 82% vitrinite and average 17.6% inertinite. The thickness and gas content of this seam range from 0.21–9.87 m (avg. 3.26 m) and 0.49–36.80 m^3/t (avg. 20.52 m^3/t), respectively. No.15 coal seam in this area have low permeability with values of 0.001–22.12 mD (avg. 0.9 mD), and low effective porosity with values of 3.72–6.23% (avg. 4.92%). The coal permeability presents good negative correlation with burial depth. Pore structure of this seam is characterized by well-developed diffusion and adsorption pores (<100 nm) and less-developed seepage pores (>100 nm), which is favorable for gas adsorption but unfavorable for migration and output of gas.

The gas production extracted from No. 15 coal seam is generally poor and varies dramatically regionally. The impacts of seven geological factors (coal thickness, burial depth, gas content, RCPOP, porosity, permeability and hydrogeological condition) on the CBM productivity of this seam were investigated. The analyses show that both coal thickness and RCPOP present positive correlation with gas production; the CBM productivity has poor relationship with gas content in this area; pore structure, permeability and hydrogeological condition show good correlation with CBM productivity of No. 15 coal seam. The medium and high production wells in this area usually have the following conditions: coal thickness > 3 m; burial depth of 550–950 m; gas content of 15–25 m^3/t; RCPOP > 0.55; high permeability; mudstone roof; weak runoff zone of groundwater; average water rate < 6 m^3/d.

Based on AHP model, the best prospective target area for CBM production of No.15 coal seam is predicted to be in the districts of Panzhuang, Chengzhuang and south of Hudi.

Acknowledgements

This work was financially supported by the Natural Science Foundation of China (No.41802192), the National Science and Technology Key Special Project of China (No.2016ZX05044-002 and No.2016ZX05043), the Shanxi Provincial Basic Research Program—CoalBed Methane Joint Research Foundation (No.2012012001 and No.2015012014), Open Fund of State Key Laboratory of Water Resource Protection and Utilization in Coal Mining (No.SHJT-17-42.18), and the Fundamental Research Funds for the Central Universities (No.CUGL170811). We also thank the reviewers and the Editor for their helpful comments that help greatly improve the quality of the paper.

Manuscript received Jan. 9, 2018
accepted Mar. 25, 2018
edited by Jeff Liston and Fei Hongcai

References

Ayers, W.B.J., 2002. Coalbed gas systems, resources, and production and a review of contrasting cases from the San Juan and Powder River basins. *AAPG Bulletin*, 86(11): 1853–1890.

Bustin, R.M., and Clarkson, C.R., 1998. Geological controls on coalbed methane reservoir capacity and gas content. *International Journal of Coal Geology*, 38(1): 3–26.

Cai, Y.D., Liu, D.M., Yao, Y.B., Li, J.Q., and Qiu, Y.K., 2011. Geological controls on prediction of coalbed methane of No. 3 coal seam in Southern Qinshui Basin, North China. *International Journal of Coal Geology*, 88: 101–112.

Chen Zhenhong, Wang Yibing, Yang Jiaosheng, Wang Xianhua, Chen Yanpeng and Zhao Qingbo, 2009. Influencing factors on coal-bed methane production of single well: A case of Fanzhuang Block in the south part of Qinshui Basin. *Acta Petrolei Sinica*, 30(3): 409–416 (in Chinese with English abstract).

Colmenares, L.B., and Zoback, M.D., 2007. Hydraulic fracturing and wellbore completion of coalbed methane wells in the Powder River Basin, Wyoming: implications for water and gas production. *AAPG Bulletin*, 91(1): 51–67.

Durucan, S., and Edwards, J.S., 1986. The effects of stress and fracturing on permeability of coal. *Mining Science and Technology*, 3(3): 205–216.

Fang Huihuang, Sang Shuxun, Wang Jilin, Liu Shiqi and Ju Wei, 2017. Simulation of Paleotectonic Stress Fields and Distribution Prediction of Tectonic Fractures at the Hudi Coal Mine, Qinshui Basin. *Acta Geologica Sinica* (English Edition), 91(6): 2007–2023.

Fu, H.J., Tang, D.Z., Xu, T., Xu, H., Tao, S., Li, S., Yin, Z.Y., Chen, B.L., Zhang, C., and Wang, L.L., 2017. Characteristics of the pore structure and fractal dimension of low-rank coal: A case study of Lower Jurassic Xishanyao coal in the middle of the southern Junggar Basin, NW China. *Fuel*, 193: 254–264.

Fu Xuehai, Qin Yong and Li Guizhong, 2001. An analysis on the principal control factor of coal reservoir permeability in central and southern Qinshui basin. *Coal geology & exploration*, 29(3): 16–19 (in Chinese with English abstract).

Fu, X.H., Qin, Y., Wang, G.G.X., and Rudolph, V., 2009. Evaluation of coal structure and permeability with the aid of geophysical logging technology. *Fuel*, 88: 2278–2285.

Harker, P.T., and Vargas, L.G., 1987. The theory of ratio scale estimation: Saaty's analytical hierarchy process. *Management Science*, 33 (11): 1383–1403.

Johnson, R.L., Flottman, T., and Campagna, D.J., 2002. Improving results of coalbed methane development strategies by integrating geomechanics and hydraulic fracturing technologies. Melbourne, Australia: *SPE Asia Pacific Oil and Gas Conference and Exhibition*, 1–13.

Kaiser, W.R., Hamilton, D.S., Scott, A.R., Tyler, R., and Finley, R.J., 1994. Geological and hydrological controls on the producibility of coalbed methane. *Journal of the Geological Society*, 151(3): 417–420.

Kaiser W.R., and Ayers, W.B., 1994. Geologic and hydrologic characterization of coalbed-methane reservoirs in the San Juan basin. *SPE Formation Evaluation*, 9(3): 175–184.

Kharaka, Y.K., and Carothers, W.W., 1986. *Handbook of environmental isotope geochemistry*. Amsterdam: Elsevier Scientific Publishing Company.

Li, Y., Tang, D.Z., Xu, H., Elsworth, D., and Meng, Y.J., 2015. Geological and hydrological controls on water coproduced with coalbed methane in Liulin, eastern Ordos basin, China. *AAPG Bulletin*, 99(2): 207–229.

Li, Y., Zhang, C., Tang, D.Z., Gan, Q., Niu, X.L., Wang, K., and Shen, R.Y., 2017. Coal pore size distributions controlled by the coalification process: an experimental study of coals from the Junggar, Ordos and Qinshui basins in China. Fuel, 206: 352–363.

Liu Huanjie, Qin Yong and Sang Shuxun, 1998. *Coalbed Methane Geology of Southern Shanxi Province in China*. Xuzhou: China University of Mining and Technology Press, 138–140 (in Chinese).

Liu, H.H., Sang, S.X., Wang, G.G.X., Li, Y.M., Li, M.X., and Liu, S.Q., 2012. Evaluation of the synergetic gas-enrichment and higher-permeability regions for coalbed methane recovery with a fuzzy model. *Energy*, 39: 426–439.

Liu, H.H., Sang, S.X., Formolo, M., Li, M.X., Liu, S.Q., Xu, H.J., An, S.K., Li, J.J., and Wang, X.Z., 2013. Production characteristics and drainage optimization of coalbed methane wells: A case study from low-permeability anthracite hosted reservoirs in southern Qinshui Basin, China. *Energy for Sustainable Development*, 17: 412–423.

Liu Jinda, Zhao Yingchang, Liu Enkai and Wang Dongsheng, 1997. Discussion on the stable isotope time-space distribution law of China atmospheric precipitation. *Site Investigation Science and Technology*, 3: 34–39 (in Chinese with English abstract).

Lv, Y.M., Tang, D.Z., Xu, H., and Luo, H.H., 2012. Production characteristics and the key factors in high-rank coalbed methane fields: a case study on the Fanzhuang Block, Southern Qinshui Basin, China. *International Journal of Coal Geology*, 96–97: 93–108.

Mcbeth, I., Reddy, K.J., and Skinner, Q.D., 2003. Chemistry of trace elements in coalbed methane product water. *Water Research*, 37: 884-890.

Meng, Y.J., Tang, D.Z., Xu, H., Li, C., Li, L., and Meng, S.Z., 2014. Geological controls and coalbed methane production potential evaluation: a case study in Liulin area, eastern Ordos Basin, China. *Journal of Natural Gas Science and Engineering*, 21: 95–111.

McKee, C.R., Bumb, A.C., and Koenig, R.A., 1998. Stress-dependent permeability and porosity of coal and other geologic formations. *SPE Formation Evaluation*, 3(01): 81–91.

Moore, T.A., 2012. Coalbed methane: A review. *International Journal of Coal Geology*, 101: 36–81.

Pashin, J.C., 1997. Productivity of coalbed methane wells in Alabama. Tuscaloosa, Alabama, USA: International Coalbed Methane Symposium, 65–74.

Pashin, J.C., 2007. Hydrodynamics of coalbed methane reservoirs in the Black Warrior Basin: key to understanding reservoir performance and environmental issues. *Applied Geochemistry*, 22: 2257–2272.

Pratt, T.J., Mavor, M.J., and DeBruyn, R.P., 1999. Coal gas resource and production potential of subbituminous coal in the Powder River Basin. Gillette, Wyoming, USA: *SPE Rocky Mountain Regional Meeting*, 195–204.

Qin, Y., Moore, T.A., Shen, J., Yang, Z.B., Shen, Y.L., and Wang, G., 2018. Resources and geology of coalbed methane in China: a review. *International Geology Review*, 60: 777–812.

Song Yan, Liu Honglin, Liu Shaobo, Zhao Mengjun and Su Xianbo, 2010. *Coalbed Methane Accumulation Geology of China*. Beijing: Science Press (in Chinese).

Song Yan, Liu Shaobo, Ju Yiwen, Hong Feng, Jiang Lin, Ma Xingzhi and Wei Mingming, 2013. Coupling between gas content and permeability controlling enrichment zones of high abundance coal bed methane. *Acta Petrolei Sinica*, 34(3): 417–426 (in Chinese with English abstract).

Rice, C.A., 2003. Production waters associated with the Ferron coalbed methane fields, central Utah: chemical and isotopic composition and volumes. *International Journal of Coal Geology*, 56(1): 141–169.

Satty, T.L., 1990. How to make a decision: the analytic hierarchy process. *European Journal of Operational Research*, 48 (1): 9–26.

Scott, A.R., 2002. Hydrogeologic factors affecting gas content distribution in coal beds. *International Journal of Coal Geology*, 50(1): 363–387.

Su, X.B., Lin, X.Y., Liu, S.B., Zhao, M.J., and Song, Y., 2005. Geology of coalbed methane reservoirs in the Southeast Qinshui Basin of China. *International Journal of Coal Geology*, 62(4): 197–210.

Tao, S., Tang, D.Z., Xu, H., Gao, L.J., and Fang, Y., 2014. Factors controlling high-yield coalbed methane vertical wells in the Fanzhuang Block, Southern Qinshui Basin. *International Journal of Coal Geology*, 134–135: 38–45.

Walsh, J.B., 1981. Effect of pore pressure and confining pressure on fracture permeability. *International Journal of Rock Mechanics and Mining Sciences & Geomechanics Abstracts*, 18: 429–435.

Wang, B., Sun, F.J., Tang, D.Z., Zhao, Y., Song, Z.H., and Tao, Y., 2015. Hydrological control rule on coalbed methane enrichment and high yield in FZ Block of Qinshui Basin. *Fuel*, 140: 568–577.

Wang Shanbo, Tang Shuheng, Wan Yi, Li Zhongcheng and Zhang Songhang, 2013. The hydrogen and oxygen isotope characteristics of drainage water from Taiyuan coal reservoir. *Journal of China Coal Society*, 38(3): 448–454 (in Chinese with English abstract).

Wang Hongyan, Zhang Jianbo, Liu Honglin and Qin Yong, 2001. Hydrogeologic feature of coalbed methane reservoir in the southern Qinshui Basin. *Coal Geology & Exploration*, 29 (5): 33–36 (in Chinese with English abstract).

Wei, C.T., Qin, Y., Wang, G.G.X., Fu, X.H., Jiang, B., and Zhang, Z.Q., 2007. Simulation study on evolution of coalbed methane reservoir in Qinshui basin, China. *International Journal of Coal Geology*, 72(1): 53–69.

Yao, Y.B., Liu, D.M., Tang, D.Z., Huang, W.H., Tang, S.H., and Che, Y., 2008a. A Comprehensive model for evaluating coalbed methane reservoirs in China. *Acta Geologica Sinica* (English Edition), 82(6): 1253–1270.

Yao, Y.B., Liu, D.M., Tang, D.Z., Tang, S.H., and Huang, W.H., 2008b. Fractal characterization of adsorption-pores of coals from North China: An investigation on CH_4 adsorption capacity of coals. *International Journal of Coal Geology*, 73: 27–42.

Yao, Y.B., Liu, D.M., Tang, D.Z., Tang, S.H., Che, Y., and Huang, W.H., 2009a. Preliminary evaluation of the coalbed methane production potential and its geological controls in the Weibei Coalfield, Southeastern Ordos Basin, China. *International Journal of Coal Geology*, 78: 1–15.

Yao, Y.B., Liu, D.M., Tang, D.Z., Tang, S.H., Huang, W.H., Liu, Z.H., and Yao, C., 2009b. Fractal characterization of seepage-pores of coals from China: An investigation on permeability of coals. *Computers & Geosciences*, 35: 1159–1166.

Yao, Y.B., Liu, D.M., and Yan, T.T., 2014. Geological and hydrogeological controls on the accumulation of coalbed methane in the Weibei field, southeastern Ordos Basin. *International Journal of Coal Geology*, 121: 148–159.

Ye Jianping and Lu Xiaoxia, 2016. Development status and technical progress of China coalbed methane industry. *Coal Science and Technology*, 44(1): 24–28 (in Chinese with English abstract).

Ye Jianping, Peng Xiaomei and Zhang Xiaopeng, 2009. Exploration Orientation and Development Proposal of Coalbed Methane in Qinshui Basin of Shanxi Province. *China Coalbed Methane*, 6(3): 7–11 (in Chinese with English abstract).

Zhang Peihe, Liu Yuhui, Wang Zhengxi and Liu Nana, 2011. Geological factors of production control of CBM well in south Qinshui Basin. *Natural Gas Geoscience*, 22(5): 909–914 (in Chinese with English abstract).

Zhang, S.H., Tang, S.H., Li, Z.C., Guo, Q.L., and Pan, Z.J., 2015. Stable isotope characteristics of CBM co-produced water and implications for CBM development: the example of the Shizhuangnan block in the southern Qinshui Basin, China. *Journal of Natural Gas Science and Engineering*, 27: 1400–1411.

Zhang Zheng, Qin Yong, Fu Xuehai, Yang Zhaobiao and Guo Chen, 2015. Multi-Layer Superposed Coalbed Methane System in Southern Qinshui Basin, Shanxi Province, China. *Journal of Earth Science*, 26(3): 391–398.

Zhang, Z., Qin, Y., Bai, J.P., Li, G.Q., Zhuang, X.G., and Wang, X.M., 2018. Hydrogeochemistry characteristics of produced waters from CBM wells in Southern Qinshui Basin and implications for CBM commingled development. *Journal of Natural Gas Science and Engineering*, 56: 428–443.

Zhang, Z., Qin, Y., Zhuang, X.G., Li, G.Q., and Wang, X.M., 2018. Poroperm characteristics of high-rank coals from Southern Qinshui Basin by mercury intrusion, SEM-EDS, nuclear magnetic resonance and relative permeability analysis. *Journal of Natural Gas Science and Engineering*, 51: 116–128.

Zhang, S.H., Tang, S.H., Li, Z.C., Pan, Z.J., and Shi, W., 2016. Study of hydrochemical characteristics of CBM co-produced water of the Shizhuangnan Block in the southern Qinshui Basin, China, on its implication of CBM development. *International Journal of Coal Geology*, 159: 169–182.

Zou, M.J., Wei, C.T., Fu, X.H., Bao, Y., and Cai, Z.X., 2013. Investigating reservoir pressure transmission for three types of coalbed methane reservoirs in the Qinshui Basin in Shan'xi Province, China. *Petroleum Geoscience*, 19(4): 375–383.

About the first author

ZHANG Zheng Male; born in 1990 in Hebi City, Henan Province; doctor; lecturer of Faculty of Earth Resources, China University of Geosciences (Wuhan); He is now interested in the study on coal and coalbed methane geology. Email: zhangzheng@cug.edu.cn; phone: 15827275189.